Implications of Altering Signalling Pathways and Cell Morphology by Polyoma Middle-T at the Onset of Morphological Cell Changes

BY

Alexandra Eicher

Dipl. Biol. Univ.

Implications of Altering Signalling Pathways and Cell Morphology by Polyoma Middle-T at the Onset of Morphological Cell Changes

BY

Alexandra Eicher
Dipl. Biol. Univ.

Implications of Altering Signalling Pathways and Cell Morphology by Polyoma Middle-T at the Onset of Morphological Cell Changes

By

Alexandra Eicher

A Thesis

Submitted to the School of Graduate Studies

in Partial Fulfilment of the Requirements

for the Degree

Master of Science

McMaster University

MASTER OF SCIENCE (1995) McMASTER UNIVERSITY

(Biochemistry) Hamilton, Ontario

TITLE: Implications of Altering Signalling Pathways and Cell Morphology by Polyoma Middle-T at the Onset of Morphological Cell Changes

AUTHOR: Alexandra Eicher, Dipl. Biol. Univ.
(University Erlangen-Nuremberg, FRG)

SUPERVISER: Professor David W. Andrews

NUMBER OF PAGES: xiv; 109pp.

Abstract

Subcellular localization of polyoma mT was determined by immunofluorescence microscopy, using primary monoclonal/polyclonal antibodies and secondary polyclonal antibodies conjugated with fluorescent dyes. Our results confirm and extend previous studies reporting the association of mT with an intracellular compartment. However, it is shown that the perinuclear compartment containing the bulk of mT expressed in MRC5 cells is both Brefeldin A resistant and distinct from the known compartments of the secretory pathway. The integrity of most subcellular compartments was not altered by mT expression. However, secondary lysosomes and late endosomes were reorganized in cells expressing mT. Early in cell transformation mT alters several members of the cytoskeletal array, with the most profound effects on actin. In cells coinfected with viruses encoding either mT or pp60$^{c\text{-}src}$, the areas of subcellular localization of both proteins are largely overlapping. In addition, mT recruits Shc to this subcellular localization indicating that mitogenesis as well as morphological cell transformation may be regulated from this novel intracellular compartment.

Dedication

To my parents

Acknowledgements

First of all, I would like to thank my supervisor, Dr. David Andrews for the possibility to work on this thesis, his support, encouragement and making my time in his lab an excellent learning experience.

Secondly, I would like to thank Dr. Brian Leber (M.D.) for his professional support, but also mental coaching during the time I needed it most.

Special thanks to Mina Falcone, Jason Young and Gil Abisdris for their friendship, personal support, discussions and their ability to always be there when help was needed.

I would also like to thank Josie Ursini, Glen Vance and Fabiola Janiak for their friendship and support.

Finally, I would like to thank Barb, the whole McWhinney clan, Louise and Dave for their friendship, their endless support and for always being there for me.

Table of Contents

List of Figures

List of tables

List of Abbreviations

BFA	Brefeldin A
C-terminus	Carboxyl-terminus
EGFR	Epidermal growth factor receptor
ER	Endoplasmic reticulum
ERGIC	ER-Golgi intermediate compartment
Fig.	Figure
FITC	Fluorescein isothiocyanate
Grb2	growth factor receptor bound protein 2
Gst	Glutathione-S-transferase
IP	Inositol phosphate
LRSC	Lissamine rhodamine sulfonyl chloride
mT	Polyoma middle T (tumor) antigen
N-terminus	Amino-terminus
PBS	Phosphate buffered saline
PDGF	Platelet derived growth factor
PFU	Plaque forming units
PI3-K	Phosphatidylinositol 3-kinase
PIP	Phosphatidylinositol phosphate
PLC	Phospholipase C
PP2A	Phosphatase 2A
Shc	Src homologous and collagen protein

Sos	homolog of the Drosophila guanine-nucleotide-exchange factor
SDS-Page	Sodium dodecyl sulphate polyacrylamide electrophoresis
Tab.	Table
TGN	Trans-Golgi network
TRITC	Tetramethylrhodamin isothiocyanate
TRSC	Texas Red sulfonyl chloride
Tyr	Tyrosine

1. Introduction

Transformation of cells from a normal to a tumorigenic phenotype is a complex process, which involves many incompletely understood intra-cellular and extracellular events. Cell transformation can be caused by a variety of agents such as chemical carcinogens, radiation, and DNA- and RNA-viruses. Early gene products of members of a DNA virus group - the papovavirus group - have been found to transform cells (1). The papova virus group includes viruses such as simian virus 40 (SV40), baculo virus (BK-virus) and polyoma virus (1). Specifically, for polyoma virus, the middle T (tumor) antigen (mT) has been found to be involved in transformation of a wide variety of cells (1, 2, 32). Expression of mT is sufficient to transform established cell lines and a variety of tissues (3, 4, 5, 36, 86). In transgenic mice mT induces tumors like salivary gland adenocarcinoma, thyroid adenocarcinoma, mammary carcinoma and liver haemangioma (87). Inducible cell transformation by mT is therefore an excellent model system for investigating the components of this process.

1.1 Characteristics of transformed cells

Transformed cells in tissue culture are defined by several key features (reviews 1 & 90). The most notable characteristics of transformed cells that distinguish them from normal cells are alterations in cell morphology and unregulated cell division.

1.1.1 Cell morphology

Three different classes of filamentous assemblies (microfilaments, intermediate filaments and microtubules) form the cellular cytoskeleton, which is responsible for cell shape, vesicle transport and cell migration. Cellular shape changes are due to alterations in one or more components of this intracellular cytoskeletal network. In untransformed anchorage dependent mammalian cells such as fibroblasts, DNA synthesis and growth control is usually dependent on the cell shape (91, 64). In contrast, transformed fibroblasts exhibiting spheroidal cell morphology have lost the capacity for growth arrest, dependence on anchorage for growth and contact inhibition (reviewed in 1, 90, 91).

The first class of filamentous assembly important in determining cell morphology is a structural network consisting of microfilaments and adjacent proteins. Microfilaments are polymers composed of actin subunits (90, 91). Actin is a globular protein with a molecular weight of 42 kDa. The actin binding protein α-actinin crosslinks actin filaments to stress fibres (90, 92). In normal non-muscle cells, actin filaments are found as stress fibres and as a filament network beneath the plasma membrane (91). In cellular focal adhesions actin filaments are connected via the proteins α-actinin, vinculin, and talin to the cytoplasmic domains of the transmembrane adhesion proteins of the integrin protein family (92, 93). Actin stress fibres are therefore connected through integrins to the plasma membrane and also linked to extracellular matrix proteins such as fibronectin and vitronectin (92, 93).

There is evidence that the rounded morphology of transformed fibroblasts is due to a reduced amount or total loss of actin filaments (102, 103). Loss of actin stress fibres can coincide with a loss in fibronectin binding capacity and therefore decreased adhesiveness to the substrate (91). In addition, transformed cells are also found to lack or have reduced amounts of surface fibronectin (103, 91). Furthermore, transformed cells are found to secrete plasminogen activator (reviewed in 90). Plasminogen activator is a protease capable of converting plasminogen, a protein contained in serum, into the serine protease plasmin, which also contributes to cell shape changes by lysing extracellular matrix proteins (90). In normal cells, protease treatment has also been implicated in loss of actin filaments (90). Finally, in Rous sarcoma virus (RSV) transformed cells with cytoskeletal alterations, vinculin, a protein important in linking actin stress fibres to focal adhesion plaques, was shown to be a target of $pp60^{c\text{-}src}$ (94). Other putative $pp60^{c\text{-}src}$ cytoskeletal substrates might be involved in the process (78, 79). Taken together, these results suggest that alterations in components of the microfilament cytoskeleton contribute to cellular morphology changes that accompany cell transformation.

The second class of filamentous assembly important in determining cell morphology is a structural network consisting of microtubules. Microtubules are formed from a helical array of α- and β-tubulin heterodimer subunits (90). Both α- and β-tubulin are globular proteins with a molecular weight of 50 kDa. In fibroblasts microtubules are involved in determination of cell morphology, mitosis, organelle movement, and in translocation of secretory

vesicles (reviewed in 90, 91). Normal cells are thought to contain twice as much tubulin as transformed cells (104). However, this observation as well as reports of alterations in the organization of microtubules after cell transformation is controversial (104, 105, 106). Some report a difference in the organization or amount of microtubules (104, 106) while others do not (102, 105).

In contrast to microfilaments or microtubules, the third class of filamentous assembly, intermediate filaments, are reported to maintain structural properties in transformed cells (91). The intermediate filaments in fibroblasts are composed of units of the protein vimentin (reviewed in 90, 91). Two units of vimentin form a coiled coiled dimer. Antiparallel aggregation of two dimers then form a tetramer, which subsequently polymerizes with other tetramers to a protofilament. Finally, eight protofilaments form a cylindrical intermediate filament (90). Intermediate filaments span cells from the nucleus to the plasma membrane and are often found to be associated with microtubules (90, 91).

The alterations in the intricate cytoskeletal structural network responsible for changes in cell morphology seen in transformed cells are most pronounced for microfilaments, but little is known about the mechanism that mediates this effect.

1.1.2 Mitogenic signalling

The second overall aspect of cell transformation is the alteration of normally

regulated signal transduction pathways that initiate cell division. In untransformed cells, these pathways transmit signals originating from extracellular mitogenic stimuli (hormones, growth factors) through receptors located in the plasma membrane via recruitment and phosphorylation of cytoplasmic protein substrates, production of secondary messengers to the nucleus or other cytoplasmic targets (reviewed in 88). This results in a pleiotropic cell response necessary for cell differentiation, controlled cell division, growth and behaviour (88). Alteration of these strictly regulated signal transduction pathways can cause cell transformation (88).

As a result transformed cells require lower concentrations of growth factors and hormones for continued cell growth. Some cells are even found to produce and release their own specific growth factors (90).

The transforming protein of polyoma virus (mT) is believed to cause cell transformation by associating with members of the signalling pathways. It has been suggested, that "mT transforms cells by acting as a functional homologue of an activated tyrosine kinase-associated growth-factor receptor" (27).

1.2 Polyoma virus and its encoded proteins

The polyoma virus is a member of the papovavirus group, which also includes simian virus 40 (SV40, host: monkey) and the baculo virus (BK-virus, host: insects) (1). Mice are the natural hosts of the polyoma virus, and cells from other rodents have been classified as permissive, semipermissive or nonpermissive (1). Only mouse cells are fully permissive for infection:

upon infection, cells support viral DNA replication, produce proteins necessary for virus packaging, are lysed and release large quantities of virus particles (1). Upon infection of semipermissive hamster cells, only a few cells produce low yields of virus. In contrast, nonpermissive rodent cells lines (e.g some rat cells) express the early T-antigen proteins upon virus infection, and a small number of cells undergo changes resulting in cellular immortalization or transformation (1).

The polyoma virus genome consists of a small, double stranded , closed circular DNA. The reading frames of the six known proteins are partly overlapping. The early genes (transcribed prior to the onset of viral DNA replication) encode three proteins known as the large (785 amino acids), middle (421 amino acids) and small (195 amino acids) T (tumor) antigens (1, 32). All three T-antigens are encoded in the same area of the genome and have a common N-terminus (1). However, differential splicing of the messenger RNA causes different reading frames for translation, and all three T-antigens possess unique sequences at the C-terminus (1). The remaining three proteins are the late capsid proteins VP1, VP2, and VP3 (1, 2).

In infected cells, the function of small T-antigen (sT/22kDa) is not yet determined. However, primary sequence similarities between sT and some hormones, e.g. glycoprotein hormones such as thyroid-stimulating hormone, have been found (1). Large T-antigen (lT) is predominantly located in the nucleus, where it controls cellular and viral DNA/RNA synthesis, and is important for cell immortalization (1, 32). In infected and transformed cells,

lT is observed to be highly modified by phosphorylation (1). The various molecular weights (88 kDa-100 kDa) observed may be explained by different modifications of lT; these modifications may confer functional specificity in vivo (1).

The viral protein involved in cell transformation is the middle T antigen (mT) (1, 2, 32). Expression of mT causes key characteristics of transformed cells in established cell lines, such as anchorage independent growth of cells in agar, lower cellular contact inhibition, disruption of cytoskeletal structures and subsequently changes in cell morphology (1). Furthermore, expression of mT is sufficient to transform a variety of tissues, and causes tumors in transgenic mice (3, 4, 5, 36, 86, 87). MT is a phosphoprotein of 421 amino acids with a calculated molecular weight of 49 kDa (1). However, mT usually migrates in SDS-PAGE as a 56 KDa or 58 kDa protein (1). The two forms differ in their pattern of serine phosphorylation in the C-terminus (1). Approximately 30% of the amino acids of mT are hydrophobic, and the amino acid residues near the C-terminus are arranged in a sequence present in a large number of transmembrane proteins (1). A continuous hydrophobic stretch spanning 22 amino acids (amino acids 394-415) is flanked by several positively charged amino acids such as lysine and arginine (1, 33). Proteins, including mT, which lack a N-terminal signal sequence, but contain this C-terminal motif (termed an insertion sequence), are proposed to spontaneously associate with membranes post-translationally (60). In mT, truncation or mutation of this region result in loss of both mT

membrane attachment and cell transformation (32, 33). No intrinsic enzymatic activity has been detected for mT (1, 2, 32). However, mT associates with members of signalling pathways including tyrosine kinases (2, 8-15, 65), a phosphatidylinositol kinase (16, 17), a phosphatase (23, 24), the recently characterized adapter molecule Shc (27, 71), and some isoforms of the 14-3-3 protein family (57). Mutational analysis of mT has shown that if some of these specific protein interactions are missing, mT is no longer able to transform cells in tissue culture (31). Therefore, specific mT-protein interactions are believed to be responsible for transformation (31, 32).

1.3 Polyoma middle T binding proteins

1.3.1 Src family kinases

The protein tyrosine kinase activity associated with mT results from the binding of one or more members of the src family of tyrosine kinases. At present there are nine known members of the src gene family, and fourteen different src related gene products. All these proteins are tyrosine kinases and three members of this family, $pp60^{c\text{-}src}$, $pp60^{c\text{-}yes}$ and $pp59^{c\text{-}fyn}$, have been found to associate with mT in cultured cells (2, 8-15, 65).

All Src-protein family members contain the following conserved regions: (a) a N-terminal myristoylation signal, (b) Src homology (SH) 3, (c) SH2 regions, (d) a kinase (SH1/catalytic) domain and (e) a C-terminal non-catalytic tail (65). In $pp60^{c\text{-}src}$ the initiator amino acid methionine is absent and a N-terminal glycine is fatty acylated with myristic acid. Myristoylation is

essential for pp60$^{c\text{-}src}$ membrane binding.

SH3 domains contain ~60 amino acids and are present in protein families otherwise unrelated to each other. A large number of SH3 containing proteins are associated with membranes, suggesting that SH3 domains are involved in subcellular localization (73). In addition, a role in regulating protein-protein interactions during signalling has been indicated (66, 67). Specificly, the SH3 domain of pp60$^{c\text{-}src}$ mediates the recruitment of substrates to this protein tyrosine kinase (68).

The SH2 domain region (~100 amino acids) of src family tyrosine kinases shares high homology with other tyrosine kinases, and is present in many signalling proteins (30, 67, 68). SH2 domains bind to phosphorylated tyrosine residues with high affinity (68). The sequence of three residues immediately C-terminal to the phospho-tyrosine determines the binding specificity for different SH2 domains. SH2 domains are thought to regulate protein-protein interactions during signal transduction by binding to specific tyrosine phosphorylated sites on growth factor receptors and cytoplasmic proteins (67, 68).

Within the catalytic ATP binding site of the SH1 domain of pp60$^{c\text{-}src}$, a lysine residue (lys 295) has been found to be essential for the proteins kinase activity (95). The lysine residue is conserved in all known protein kinases containing this motif (95). It has been proposed that "the primary amino group of lysine carries out the specialized function of proton exchange in the phosphotransferase reaction" (95).

The amino terminal region of mT interacts with the fifteen carboxy-terminal amino acids of the non-catalytic tail of pp60$^{c\text{-}src}$ and thereby prevents phosphorylation of tyr 527 within the C-terminus (5, 9, 58). An increase in pp60$^{c\text{-}src}$ kinase activity is correlated with dephosphorylation of its tyrosine 527 residue. This dephosphorylation is suggested to cause conformational changes in pp60$^{c\text{-}src}$ and, subsequently, autophosphorylation of Tyr-416 (part of the catalytic domain) which results in a stimulatory effect on the kinase activity (65).

As a consequence of association with mT, three members of the Src family (pp60$^{c\text{-}src}$, pp60$^{c\text{-}yes}$ and pp59$^{c\text{-}fyn}$) undergo autophosphorylation and subsequently phosphorylate mT *in vitro* (22). Activation of one or more src family kinases has been suggested to be necessary, but not sufficient for mT mediated cell transformation (65, 9). Previously published data indicate that, if necessary, pp60$^{c\text{-}src}$ kinase activity can be compensated by residual levels of Yes, Fyn kinase activity and phosphatidylinositol 3-kinase (PI3-K) activity in some cells (22). In immortalized pp60$^{c\text{-}src}$-negative fibroblasts, the formation of foci on cell monolayers and colony formation in soft agar were both induced by mT. The level of mT phosphorylation in pp60$^{c\text{-}yes}$ and pp59$^{c\text{-}fyn}$ immunoprecipitates in pp60$^{c\text{-}src}$-positive or negative cell lysates did not change. However, mT associated PI3-K activity was reduced 30-60% in pp60$^{c\text{-}src}$-negative cells (22).

Activation of src family non-receptor tyrosine kinases results in the phosphorylation of tyrosine residues (297, 250, 315 and 322) of mT. The

phosphorylated tyrosine residues 250 and 315 of mT are the major sites for interaction with other proteins (97).

Another signalling pathway, that may be altered by mT via pp60$^{c\text{-}src}$, is the inositol lipid pathway. Activation of pp60$^{c\text{-}src}$ after complex formation with mT leads to elevated levels of inositol 1,4,5-trisphosphate (IP_3). Hence the activation of phospholipase C may be a direct or indirect consequence of pp60$^{c\text{-}src}$ activation (21).

Phospholipase C is a critical regulator of the inositol lipid pathway. After activation, the enzyme hydrolyses phosphodiesterbonds that link phosphorylated inositol units to acetylated glycerol moieties (phospholipids of plasma membrane). The resulting IP_3 and diacylglycerol (DAG) act as second messengers: IP_3 opens Ca^{2+} channels thereby increasing cytoplasmic Ca^{2+} levels, and DAG activates protein kinase C (PKC) (72).

1.3.2 Phosphatidylinositol 3-kinase

Phosphorylation of mT tyrosine 315 enables mT to bind to the N-terminal SH2 domain of the 85 kDa regulatory subunit of phosphatidyl-inositol 3-kinase (PI3-K) (16-20). In normal cells PI3-K is a heterodimer consisting of a 85 kDa regulatory and a 110 kDa catalytic subunit. The regulatory subunit is a multidomain protein containing an N-terminal SH3 domain, followed by a region with homology to the breakpoint cluster region gene (Bcr), and two SH2 domains which are separated by a previously characterized inter-SH2 region (20, 69). The Bcr gene is located on

chromosome 22 and has been shown to encode a 160 kDa phosphoprotein (112). Regions with homology to Bcr are also found in proteins that interact with and activate GTPases, suggesting that the regulatory subunit of PI3-K may also have a role in activating such proteins. The C-terminal region of the 110 kDa catalytic subunit shares significant sequence homology with the Saccharomyces cerevisiae VPS34 gene product, which is implicated in vacuole sorting, suggesting a possible role for PI3-K in membrane trafficking and vesicle morphogenesis (69,70). PI3-K associates with both receptor and nonreceptor tyrosine kinases involved in growth and transformation. Recent data demonstrate that binding of consensus sequences containing phosphorylated tyrosine to either the N- or C-terminal SH2 domain of the regulatory 85 kDa subunit generates an intramolecular signal propagated through a 102 amino acid segment of the inter-SH2 region to allosterically activate the 110 kDa catalytic subunit (19, 20). This kinase attaches a phosphate group to the 3'-hydroxyl group of the inositol ring of phosphatidylinositol (PI) and/or its phosphorylated derivates phosphatidyl-inositol 4-phosphate (PI-4-P) and phosphatidylinositol 4,5-bisphosphate (PI-4,5-P_2) (16, 20, 96). These substrates are generated during signal transduction by phosphorylation of the 4'-hydroxyl and 5'-hydroxyl groups of the phosphatidylinositol ring (PI) of some plasma membrane phospholipids (72). This modification generates three novel polyphosphoinositides: phosphatidylinositol 3-phosphate (PI-3-P), phosphatidyl-inositol-3,4-bisphosphate (PI-3,4-P_2) and phosphatidylinositol triphosphate (PIP_3/PI-3, 4, 5-P_3) (16, 96). All three are thought to act as second

messengers (16). However, the novel polyphosphoinositides are not substrates of any known phospholipase Cs (96, 99). It was therefore suggested that the novel polyphosphoinositides either act directly as second messengers as part of a novel signalling pathway or are substrates for a phospholipase D (99). Phospholipase D would then be capable of hydrolysis of the phosphorylated inositol units bound to the acetylated glycerol moieties (phospholipids of plasma membrane) and generate the inositol phosphate (IP) derivates IP_4, IP_5 and IP_6 (99).

In transformed cells PI3-K associates with mT-pp60$^{c\text{-}src}$ complexes in which mT is phosphorylated at Tyr 315 and produces elevated levels of these three polyphosphoinositides (16, 96). Accumulation of these phosphatidylinositol phosphates correlates with cell growth and transformation *in vivo* (16). Only mT-pp60$^{c\text{-}src}$ complexes associated with PI3-K are implicated in full cell transformation (21). Therefore, complex formation of PI3-K with mT is necessary, but not sufficient for cell transformation (16, 21, 95).

1.3.3 Phosphatase 2A

Another protein which associates with mT is phosphatase 2A (PP2A). However, whether or not this association plays an important role in mT cell transformation has yet to be determined. PP2A is an abundant cytoplasmic serine/threonine protein phosphatase that regulates glycolysis, gluconeogenesis, fatty acid breakdown and amino acid breakdown. It consists of a 34-37

kDa catalytic subunit, a 58-69 kDa regulatory subunit and a 54, 55 or 72 KDa regulatory subunit (24, 31). Like $pp60^{c\text{-}src}$, PP2A also interacts with the amino terminal regions of polyoma mT (23, 25). As shown by monoclonal antibodies with well defined epitopes on mT, PP2A and $pp60^{c\text{-}src}$ occupy distinguishable, though, partly overlapping regions at the N-terminus of mT (25). Nevertheless, PP2A/mT complexes and PP2A/mT/src family kinase complexes are found in both transformed and infected cells, and exhibit phosphoseryl protein phosphatase and/or tyrosine protein kinase activities (24).

1.3.4 Shc

The adapter protein Shc (Src homologous and collagen protein) also binds to mT (27). The Shc cDNA encodes two overlapping proteins with predicted molecular weights of 46.8 and 51.7 kDa (26). However, in a wide variety of cells antibodies to Shc recognize proteins with three different sizes: 46 kDa, 52 kDa and 66 kDa (26, 27). p46 and p52, which differ at their N-termini, are likely products of translation initiation at different sites (26). The variably expressed 66 kDa protein is thought to be encoded by the same gene, though, by a different distinct Shc transcript (26). Shc was found to consist of a C-terminal SH2 domain and an adjacent glycine/proline rich motif, which contains regions of homology to the α1 chain of collagen. No catalytic domain has yet been identified (26). However, Shc was found to bind to activated epidermal growth factor receptor (EGFR), resulting in Shc phosphorylation

(71, 77). Constitutive expression of Shc leads to cell transformation (26, 27, 28). Recent results suggest the existence of a multimolecular complex consisting of mT/Src family tyrosine kinases/PI3-K and Shc in transformed cells (71). They imply that the mechanism of aberrant signal transduction induced by mT results from the mT complex acting as a functional homolog of an activated tyrosine kinase-associated growth factor receptor (27, 71).

Non-receptor tyrosine kinases of the src family associate with mT and subsequently cause phosphorylation of several mT tyrosine residues. As described in section 1.3.2, phosphorylation of Tyr 315 enables the N-terminal SH2 domain of the 85 kD regulatory subunit of PI3-K to bind to mT. Furthermore, when the NPTY^{250} (Asn-Pro-Thr-Tyr) motif of mT is phosphorylated it binds to the SH2 domain of Shc (27, 71). As a result Shc is tyrosine-phosphorylated by pp60$^{c\text{-}src}$ and can bind to the SH2 domain of growth factor receptor bound protein 2 (Grb2) (28, 29). The SH3 domains of Grb2 connect Shc to the Ras signalling pathway through an interaction with Sos, a homolog of the Drosophila guanine-nucleotide-exchange factor (29, 30). This association with members of signal transduction pathways is consistent with earlier results, suggesting that p21$^{c\text{-}ras}$ lies downstream of mT and pp60$^{c\text{-}src}$ in the same pathway (56).

1.3.5 14-3-3 protein family

Recently some isoforms of the 14-3-3 protein family were found in a complex with mT (57). This protein family was originally thought to be brain

specific, but more recently has also been found in other tissues (58), and may have a role in the regulation of cell proliferation. 14-3-3 proteins have been suggested to mediate PKC translocation and to inhibit phospholipid/Ca^{2+}-dependent protein kinase C (PKC) (58). Recent data also demonstrate that members of the 14-3-3 protein family interact with and activate protein kinase RAF-1, which is suggested to play an important role in cell growth control, cell transformation and differentiation (108, 109).

1.4 MT localization

Most of the above mT binding proteins or proteins influenced by mT (e.g Ras, phospholipase C) are thought to be directly attached to the plasma membrane (e.g. $pp60^{c\text{-}src}$), to be recruited to the plasma membrane by growth factor receptors (Shc, PI3-K, PP2A) or to be located in close proximity of the inner surface of the plasma membrane (e.g Ras [29, 100], Grb2, Sos [28, 29]). With most of its target proteins thought to be close to the plasma membrane, early studies in lytically infected or transformed cells always inferred that mT was attached to the plasma membrane (49, 50, 85). This was further supported by the notion of mT being a membrane attached protein on the basis of its amino acid sequence of the C-terminus (1, 33, 59, 60), However, recent results have cast doubt on this model. In contrast to early results obtained by biochemical approaches employing different cell fractionation techniques (49, 50, 85), recent studies in lytically infected or transformed cells employing indirect immunofluorescence and immunoelectron microscopy support an

association of mT with intracellular structures such as the endoplasmic reticulum (ER) and the Golgi apparatus (34, 110). Furthermore cell fractionation in non-ionic detergents implicated different mT-sub-populations (63). One of these sub-populations was extractable together with the microtubule network (63). We recently reported that after cell fractionation the majority of mT is found in fractions enriched for membrane skeleton in mT transformed Rat-2 cells, suggesting a direct role for mT in the alterations in cellular morphology that accompany cell transformation (3).

However, all the above studies that localize mT to membranes have been carried out in cell lines which are lytically infected or transformed. It is not known what impact morphological transformation has on cellular mT distribution. Ideally one would like to examine mT localization before transformation occurs in an otherwise normal cell.

1.5 New approach in mT localization

To study the initial site of subcellular localization of mT at the onset of cell transformation, we developed a novel cell system. This novel cell system uses essentially normal embryonal, human kidney fibroblasts (MRC5). The cells are infected with a viral vector encoding mT antigen. Because the gene inserted encoding the mT antigen sequence replaces part of the early E1A and E1B regions of the adenovirus vector used (35, 55), virus replication is defective, but expression of the early region of the viral vector permits expression of the encoded protein after cell infection. By controlling cell

infection we were able to express large enough quantities of mT protein to detect it by indirect immunofluorescence and immunoblotting. In addition to localizing mT at the onset of the morphological alterations that accompany transformation, we could also assess mT interference in both aspects of cell transformation, namely alteration of cell morphology at the site of its initial localization and interaction with mitogenic signalling pathways. Evidence is provided that the observed morphological alterations in cells infected with the viral vector encoding mT are specific for mT. We demonstrate that perinuclear mT localization at the onset of the morphological alterations that accompany transformation, is different from compartments of the secretory vacuolar system and endosomes. In addition, the results demonstrate that mT alters cytoskeletal elements at this perinuclear localization, partially co-localizes with $pp60^{c\text{-}src}$ in coinfected cells and recruits Shc from the cytoplasm to this location.

2. Material and Methods

2.1 Biological reagents

Embryonal human kidney fibroblasts (MRC5) and human kidney cells (293 N3S) were provided by F. Graham, McMaster University. Adenovirus vectors, the first encoding polyoma virus middle T-antigen (Ad5/mT), the second encoding the rabies virus G-protein (Ad5/Gp) and the third encoding the proto-oncoprotein $pp60^{c\text{-}src}$ (Ad5/c-src), were provided by L. Prevec and J. Hassell, McMaster University. All viruses were propagated in 293 cells, harvested 48 to 72 h afterwards and then titered.

Polyclonal antiserum was raised against a fragment of mT from amino acids 176 to 393, as described previously (3). Immunoaffinity purified antibodies from this antiserum were prepared as described in 2.2. Monoclonal antibodies 421, 422, 721 and 722 to mT were generously provided by S. Dilworth, Royal Postgraduate Medical School, University of London, England. Monoclonal antiserum to the rabies virus G-protein was a gift from L. Prevec, McMaster University and A. Wandeler, Animal Disease Research Institute, Nepean, Ontario, Canada. Monoclonal antibodies (mAbs) against the ER-Golgi intermediate compartment marker ERGIC-p53, and polyclonal antisera to the cation-independent mannose-6-phosphate receptor (CI-MPR), antibodies to the zeta and epsilon form of the 14-3-3 protein family, the endosomal marker LE, the trans Golgi marker TGN-38, the Golgi apparatus marker mannosidase II, the adapter protein Shc and the ER marker calnexin

were provided by J.J.M. Bergeron, McGill University, Montreal, Quebec, Canada. Polyclonal antibodies to the Golgi marker β-COP were provided by J. Lippincott-Schwartz, National Institute of Health, Bethesda, Maryland. Monoclonal antiserum to the proto-oncoprotein pp60$^{c\text{-}src}$ was a gift from J.S. Brugge, Howard Hughes Medical Institute, University of Pennsylvania, Philadelphia, Pennsylvania. The polyclonal antiserum to the ER marker oligosaccharyl transferase was provided by R. Gilmore, University of Massachusetts Medical School, Worcester, Massachusetts. Polyclonal rabbit antibody to the α- and β-subunit of the signal recognition particle receptor (SRβ) was generated using conventional methods. Monoclonal antibody to the α-subunit of the signal recognition particle receptor (SRα) was kindly provided by P. Walter, Department of Biochemistry and Biophysics University of California, Medical School San Francisco, California. Polyclonal antibody to the α- and the β-subunit of the signal sequence receptor (SSRα and SSRβ) were a gift from Dr. E. Hartmann, Institut fuer Molekularbiologie, Berlin, Germany. Antisera to full-length PI3-K and the SH2 domain were a generous gift from B. Schaffhausen, Tufts University, Boston, MA. Antibodies to Phosphastase 2A (PP2A), and the SH3 domain of PI3-K were purchased from UBI, Lake Placid, N.Y.

Tetramethylrhodamine isothiocyanate (TRITC) conjugated phalloidin was obtained from Sigma Chemical Co., St.Louis, MO. Anti-β-tubulin (clone

KMX-1) and anti-vimentin (clone V9) mAbs, tropomyosin, fodrin and vinculin were purchased from Boehringer Mannheim. Secondary antibodies conjugated to Fluorescein isothiocyanate (FITC), Lissamine rhodamine sulfonyl chloride (LSRC), Texas Red sulfonyl chloride (TRSC) and alkaline phosphatase were from Jackson Immunoresearch Laboratories.

Brefeldin A was purchased from Epicenter Technologies and stored as a 5mg/ml stock solution in ethanol at -20^{0}C.

2.2 Immunoaffinity purification of polyclonal anti-middle T serum

The rabbit polyclonal antiserum to amino acids 176-393 of mT was purified by incubating the crude antiserum with protein coupled to Sepharose beads. The full protocol is described in appendix 5.1.

2.3 Determination of virus titer by plaque assay

293 N3S cells were cultured in Minimal Essential Medium (α-MEM) supplemented with 10% newborn calf serum, penicillin, streptomycin at 37^{0}C in 5% CO_2. After 24 h, virus was serially diluted (10^{-1} to 10^{-8}) in phosphate-buffered saline^{++} (PBS^{++}: PBS [25x: 5 M NaCl, 67 mM KCl, 36 mM KH_2PO_4, 130 mM Na_2HPO_4], 0.68 mM $CaCl_2$, 0.5 mM $MgCl_2$). Cells grown to ~ 80% confluence (visual assessment) in 60 mm dishes were infected with 0.2 ml of the viral dilutions in triplicate. Viral adsorption was carried out for 45 min at 37^{0}C in 5% CO_2, rocking the plates twice. After adsorption 10 ml of overlay medium equilibrated to 44^{0}C was added to each dish (overlay: 1x F11^{+++} supplemented with 5% horse serum and 0.5% agarose; F11^{+++} : F11, 1% penicillin/strepto-mycin [100x stock-solution: 16.75 mM Penicillin/ 3.43 mM Streptomycin-sulfate], 1% L-glutamine [100x: 200 mM L-glutamine] and 0.05% yeast extract). The overlay was allowed to set, and the dishes were then incubated for 6-8 days at 37^{0}C in 5% CO_2. The viral titer was determined by counting the number of plaques per dish for the entire dilution series.

2.4 Immunofluorescence

Cells were cultered in α-MEM supplemented with 10% fetal calf serum, penicillin, streptomycin and Fungizone (GIBCO) at 37°C in 5% CO_2. 24-36 h before infection cells were plated on glass coverslips and grown to ~ 40% confluence. If not otherwise stated, all cell confluence statements are visual assessments of cell density in 100 mm tissue culture dishes and are probably accurate ± 10%.

Cells were infected with either 5.6 x 10^8 PFU of Ad5/mT, Ad5/c-src or Ad5/Gp per 100 mm dish. After viral adsorption for 45 min at 37°C in 5% CO_2, cells were incubated in α-MEM with 2% horse serum.

For further analysis the glass coverslips were transferred to six-well plates, washed twice with phosphate-buffered saline, and fixed for 30 min in 4% paraformaldehyde at 24°C. After washing once with PBS, cells were permeabilized by 1% Triton X-100 in PBS for 10 min. Cells were washed with 0.02% Tween 20 in PBS for 5 min, and then blocked with 1% Bovine Serum Albumin (BSA)/0.02% Tween 20 in PBS. Primary antibodies against specific cell compartment markers were used at different dilutions (3% BSA in PBS) for 1 h at 37°C as described in Table I. After a 5 min wash with 1% BSA/0.02% Tween 20 in PBS, the cells were incubated with secondary antibodies against mouse or rabbit, which were conjugated with FITC, LSRC or Texas Red. All secondary labeled antibodies were diluted 1/30 with 3% BSA in PBS. Cells incubated only with secondary antibodies resulted in negligible signals. Actin staining was performed with TRITC-conjugated phalloidin in 3% BSA/PBS.

Table I. Primary antibodies and dilutions used in indirect immunofluorescence studies.

Marker	Dilution
mT (polyclonal affinity purified)	1/30
721/722 rat anti-mT	1/2
Gp	1/30
SSRα, SSRβ, SRα(pAb, mAb), SRβ	1/20
oligosaccharyl transferase	1/60
calnexin	1/30
calnexin (affinity purified)	1/30
β-COP	1/2000
mannosidase II	1/1000
p53	1/60
TGN-38	1/60
CI-MPR	1/1000
LE	1/100
PP2A	1/20
PI3-K: SH2 (p85) & full length	1/15
PI3-K: SH3 (p85)	1/30
14-3-3: zeta (ζ) & epsilon (ε) isoforms	1/30
$pp60^{c\text{-}src}$	1/30
Shc	1/160
β-tubulin	1/60
vimentin	1/60
vinculin	1/60
tropomyosin	1/60
fodrin	1/20

After antibody incubation, cells were washed with 0.02% Tween 20/PBS for 5 min, and then with PBS for 5 min. Finally the coverslips were dried at 37°C for 45 min before mounting in a solution of 80% glycerol and 2.5% Dabco quencher in PBS.

For Brefeldin A assays, cells were treated with 5μg/ml of BFA for 45 min prior to preparation for immunofluorescence. Coverslips were then transfered to 6 well dishes, fixed with 4% paraformaldehyde for 30 min, and further processed as described above. As a positive control for BFA, one slide of uninfected cells was stained with antibodies to β-COP.

To obtain cytoskeletal preparations, the coverslips were washed twice with cytoskeletal stabilizing buffer (CSB: 4 M glycerol, 25 mM PIPES pH 6.9, 1 mM EGTA, and 1 mM $MgCl_2$). A subsequent incubation in the same buffer containing 0.2% Triton X-100 at 24°C for 5 min permeabilized the cells and extracted soluble cell contents (73). The resulting coverslips were washed twice for 5 min in PBS, and then processed as above for fixation and staining without the permeabilization step. To rule out differences in cell infection, coverslips with adherent fibroblasts were taken from the same dish and each was then treated with antibodies against the different cytoskeletal markers.

2.5 Confocal laser scanning microscopy and image processing

Immunofluorescence data were analyzed by confocal laser scanning microscopy (LSM 10 BIOMED/Zeiss). For FITC-excitation an external Argon

laser (488 nm) was used; for LSRC- and Texas Red-excitation internal Helium/Neon laser (543 nm) were used. In addition, a barrier filter for 515 - 565 nm for the external laser and 575 - 640 nm for the internal laser were employed. Upper and lower optical sections of the cells were discarded; only sections representing the inner cell layers were used for analysis. The collected images were further processed with Vidas software 2.1 (Kontron Inc.) and Image I software (Universal Imaging Corporation). If not otherwise stated, all image scale bars in the following study indicate 25 μm.

2.6 Membrane preparation

Cells were maintained in α-MEM supplemented with 10% fetal calf serum (MRC5) or 10% newborn calf serum (293 N3S), penicillin, streptomycin and Fungizone (GIBCO) at 37^{0}C in 5% CO_2. For expression of mT or the rabies G-protein, the cells were infected with either 5.6 x 10^8 PFU of Ad5/mT or Ad5/Gp per 150 mm dish at ~ 70% confluence. After viral adsorption for 45 min at 37^{0}C in 5% CO_2, the cells were incubated with Minimal Essential Medium (α-MEM) supplemented with 2% horse serum.

293 N3S-cells were harvested at 20 h, MRC5-cells at 40 h post infection and uninfected cells at ~ 80% confluence, washed twice in PBS, resuspended in hypotonic buffer (10 mM HEPES [N-2-hydroxyethylpiperazine-N`-2-ethane-sulfonic acid, pH 7.8], 15 mM KCl, 2 mM $MgCl_2$, 0.1 mM EDTA, 1 mM

dithiothreitol, 1 mM phenylmethylsulfonyl fluoride, 0.1 μg of chymostatin per ml, 0.1 μg of antipain per ml, 0.1 μg of leupeptin per ml, 0.1 μg of pepstatin per ml, 1 U of aprotinin per ml) and incubated on ice for 10 min. After cell disruption with a homogenizer (~30 strokes) at 4°C, cell nuclei were pelleted by a centrifugation step at 1,000 x g for 5 min, 4°C. The supernatant was then centrifuged at 100,000 x g and the resulting pellet (P100) containing membranes was resuspended in a buffer containing 50 mM triethanolamine (pH 8.0) and 250 mM sucrose. The protein content was determined by the Bradford assay (following manufacturers instructions, 111). Aliquots of the supernatant (S100) and P100 solution were stored at -70°C.

2.7 Phase partitioning

For phase separation of proteins from P100 fractions, 50 μg (~25 μl) of protein was added to 100 μl of 2 x solubilisation buffer (20 mM Tris-HCl [pH 7.4], 300 mM NaCl, 2% Triton X-114, 10% glycerol) and protease inhibitors (0.1 μg of chymostatin per ml, 0.1 μg of antipain per ml, 0.1 μg of leupeptin per ml, 0.1 μg of pepstatin per ml, 1 U of aprotinin per ml, and 1 mM phenylmethylsulfonyl fluoride). After 5 min incubation on ice, ice-cold water was added to bring the final concentration to 10 mM Tris-HCl (pH 7.4), 150 mM NaCl, 1% Triton X-114, 5% glycerol. The mixture was incubated for an additional 15 min on ice. After centrifugation at 14,000 x g for 10 min at 4°C,

the pellet containing the detergent-insoluble cytoskeleton components (Csk) was resuspended in 80 μl of SDS-Page loading buffer (20% SDS, 0.2 M Tris [pH 8.9], 4 mM EDTA, 0.02% Bromophenol blue, 20% sucrose and 0.25 M dithiothreitol).

The supernatant was layered on a cushion containing 6% sucrose, 10 mM Tris-HCl (pH 7.4), 150 mM NaCl, 0.06% Triton X-114 (TX-114), 1% glycerol and was incubated at 30°C for 3 min. After centrifugation at 735 x g for 3 min at room temperature, the pellet contains hydrophobic membrane proteins (3, 52). The aqueous phase containing luminal contents and membrane skeleton components was then removed from the cushion, additional detergent (10% TX-114) at a ratio of 1:20 (vol/vol) was added, and incubated for 3 min on ice to ensure complete solubilization of the detergent. The solution was then layered on the same cushion, incubated at 30°C for 3 min to induce phase separation, and centrifuged at 735 x g for 3 min at room temperature. The pellet containing the detergent phase was kept on ice for precipitation of hydrophobic proteins with trichloroacetic acid.

The supernatant and half of the cushion were removed, and 10% TX-114 at a ratio of 1:10 (vol/vol) was added. After incubation on ice for 3 min, the solution was layered on a new cushion, and the phases were separated and the detergent pelleted as described above. The detergent pellet of the second cushion was discarded.

The supernatant was centrifuged at 150,000 x g (28 lb/in^2 in a Beckman airfuge rotor A100/30) for one hour at 4°C. The pellet of this centrifugation

step containing the membrane skeleton was resuspended in 80 μl of SDS-Page loading buffer and designated M. The supernatant was treated with 1/2 volume of 50% trichloroacetic acid to precipitate the luminal proteins. After a 15 min incubation on ice, the mixture was centrifuged in a microcentrifuge for 15 min, 4°C and washed with an ice-cold solution containing 50% ethanol/50% ether (vol/vol) to solubilize the detergent. After a second centrifugation in the microfuge (Sorvall) for 15 min, 4°C, the pellet was resuspended in 80 μl of SDS-Page loading buffer and designated Aq.

The detergent phase of the first cushion was resuspended in 300 μl of wash buffer (10 mM Tris-HCl [pH 7.4], 150 mM NaCl), the mixture was incubated on ice for 3 min and layered on a new cushion. Additional incubation at 30°C for 3 min produced phase separation and the detergent phase containing the hydrophobic proteins, was pelleted as described above. The new detergent phase was resuspened in wash buffer and protein precipitated with trichloroacetic acid as described above. The resulting pellet was then dissolved in 80 μl of SDS-Page loading buffer (D).

2.8 Immunoblotting

20 μl of each of these fractions obtained by phase partitioning (Csk, M, Aq, D) was loaded on a 10% SDS-Page gel, electrophoretically separated (62) and transferred to a nitrocellulose membrane in a buffer containing 30 mM Tris base, 240 mM glycerol, 20% methanol (constant current, 100 mA for 1 h)

using a Hoefer semi-phor transblotter (model #TE77). The membrane was blocked for 30 min in 140 mM NaCl, 10 mM Potassiumphosphate [pH 7.4], 0.02% NaN_3 and 0.5% skim milk powder at room temperature, washed three times in wash buffer (140 mM NaCl, 10 mM Potassiumphosphate [pH 7.4], 0.02% NaN_3, 0.1% Triton X-100) and then probed for ≥ 4 hours with primary antiserum. Primary polyclonal antisera were used in polyclonal antibody buffer (0.1% Triton X-100, 560 mM NaCl, 0.02% SDS, 10 mM Potassium-phosphate [pH 7.4], 0.01% NaN_3, 1% BSA) in the following dilutions: mT: 1/1000, Shc: 1/5000, Gst: 1/1000. Primary monoclonal antiserum to the rabies G protein (dilution: 1/1000) was incubated in monoclonal antibody buffer (polyclonal buffer without SDS). After repeated washing, the filter was then incubated for at least 2 hours at room temperature with secodary antibody conjugated with alkaline phosphatase (AP) against rabbit or mouse (1/2000 dilution), and then colorimetrically developed in 10 ml of AP buffer (100 mM Tris [pH 9.5], 100 mM NaCl, 5 mM $MgCl_2$) using the substrates Nitroblue Tetrazolium Chloride (NBT) and 5-Bromo-4-chloro-3 indolylphosphate p-Toluidine salt (BCIP) according to the manufacturers instructions (Gibco BRL).

3. Results

3.1 Characterization of immunoaffinity purified anti-middle T antibody for immunofluorescence

To identify the initial site of subcellular localization of mT in non-transformed cells, MRC5 cells were infected with Ad5/mT an adenovirus encoding mT in the early region of the virus. Preliminary immuno-fluorescence results using polyclonal anti-mT serum to localize mT in Ad5/mT infected MRC5 cells indicated that the antiserum had to be further purified, because of high background staining (data not shown). The crude anti Gst-mT serum was therefore immunoaffinity purified as described in appendix 5.1.

The immunopurified polyclonal anti-mT antiserum was characterized for immunofluorescence microscopy by infecting MRC5 cells with equal amounts ($5.6x10^8$ plaque forming units [pfu]) of either the virus strain Ad5/mT or the control virus Ad5/Gp. Ad5/Gp encodes the rabies virus G-membrane protein in the early region of the adenovirus and was used as a control to address the question of anti-mT antibody crossreactivity with vector encoded proteins, other than mT, or with MRC5 cell-specific proteins. The Ad5/mT virus was kindly provided by J. Hassell, McMaster University, and the Ad5/Gp virus was a generous gift from L. Prevec, McMaster University, and A. Wandeler, Animal Disease Research Institute, Nepean, Ontario, Canada. Characteristic image overlays obtained by immunofluorescence

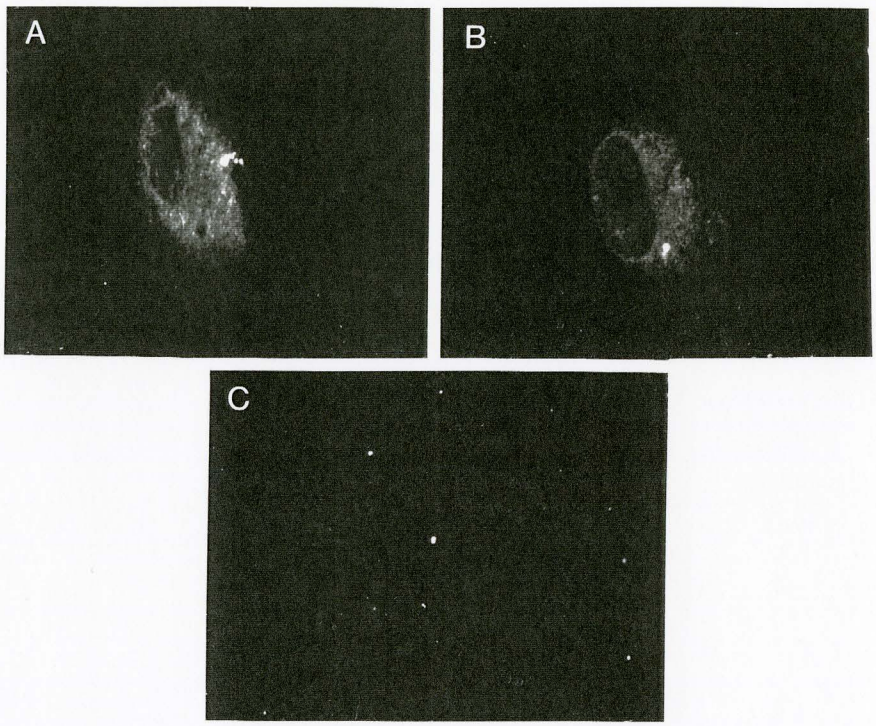

FIG. 1. Characterization of immunopurified polyclonal mT antibody through immunofluorescence localization of mT in infected MRC5 cells by confocal microscopy. MRC5 cells were grown to 40% confluency and infected with same amounts ($5.6x10^8$ plaque forming units [pfu]) of either Ad5/mT or Ad5/Gp and prepared for immunofluorescence as described in section 2.4. A) mT staining with the affinity purified anti mT antibody and B) with a mixture of two rat monoclonal antibodies (721/722) (25) in Ad5/mT infected MRC5 cells at the onset of morphological alterations as defined in section 3.2. C) Staining of Ad5/Gp infected MRC5 cells with polyclonal affinity purified antibody against mT. Note that center sections of each cell are shown.

confocal laser scanning microscopy using immunoaffinity purified anti-polyoma mT antigen (polyclonal), rat monoclonal antibodies 721/722 and fluorescein conjugated secondary antibodies are shown in figure 1. The monoclonal antibodies 721/722 were a gift from and characterized by S. Dilworth (25).

In MRC5 cells infected with the adenovirus strain Ad5/mT and stained using the affinity purified mT antibody intense fluorescence was observed in intracellular structures in the perinuclear area of the cells (Fig. 1.a). A similar perinuclear mT staining pattern was also observed with rat monoclonal mT antibodies (721/722). However, although not clear in photographic reproduction, the 721/722 monoclonals resulted in images with a higher background fluorescence compared to the affinity purified polyclonal antibody (Fig. 1.b). As expected, control cells infected with Ad5/Gp exhibited no visible staining with the affinity purified polyclonal mT antibody (Fig. 1.c). Therefore antigen staining in Ad5/mT infected MRC5 cells depended on expression of mT, and the mT antibody did not crossreact with either the other Ad5-vector encoded or MRC5 cell-specific proteins. If not otherwise stated, the immunoaffinity purified mT antibody was used in the following study in images representing mT staining.

3.2 Morphology and subcellular localization of mT early in the infection of non-transformed fibroblasts.

Because we wanted to study the mitogenic and morphological aspects of mT at the onset of cell transformation, stably transfected or viral infected transformed cell lines were unsuitable. Instead we chose an third alternative and used a recombinant adenovirus with a gene inserted encoding the desired protein sequence to infect non-transformed cells. Each vector inserted sequence replaces part of the early E1A and E1B regions of the adenovirus (35, 55). This replacement renders the virus replication defective, but still permits expression of the encoded protein after infection. Ad5/mT contains the coding sequence for polyoma mT antigen, Ad5/Gp the coding sequence for the rabies virus G-membrane protein and Ad5/c-src, which was also kindly provided by J. Hassell, McMaster University, the coding sequence for $pp60^{c\text{-}src}$. This way we achieved a high, but controlled rate of cell infection, and were able to express a large quantity of the encoded protein which was then detectable by indirect immunofluorescence and immunoblotting. In addition, by infecting normal embryonal, human kidney fibroblasts (MRC5) with Ad5/mT we were able to study mT localization at the onset of morphological transformation by mT. With this system we could assess whether mT influences both aspects of cell transformation, namely interfering with mitogenic signalling pathways and alteration of cell morphology, at the site of initial localization. The vector Ad5/Gp was used as a control to assess the effect of the vector expressing a non-transforming membrane protein on cell

morphology.

MRC 5 cells were infected with equal amounts ($5.6x10^8$ plaque forming units [pfu]) of the virus strains Ad5/mT and Ad5/Gp. Characteristic images of cells obtained by phase contrast microscopy are shown in figure 2. In addition, representative results obtained by immunofluorescence confocal laser scanning microscopy using immunoaffinity purified anti-polyoma mT antigen (polyclonal), anti-rabies G-protein (monoclonal) antibodies and Tetramethylrhodamine isothiocyanate (TRITC) conjugated phalloidin are shown in figure 3. If not otherwise stated, all image scale bars in the following study indicate 25 μm.

The first changes in cell morphology were detectable in MRC5 cells at 40 hours post Ad5/mT infection using phase contrast microscopy (Fig. 2.a). By this time approximately half of the cells were starting to alter cell shape. However, these changes were not present in MRC5 cells infected with the Ad5/Gp control vector (Fig. 2.b). This became even more obvious, when the morphology of cells infected with either Ad5/mT (Fig. 2.c) or Ad5/Gp (Fig. 2.d) at 50 hours post virus infection was compared. At 50 hours most of the Ad5/mT infected cells exhibited dramatic morphology changes (Fig. 2.c). In contrast, cells infected with the contol vector still had a normal cell shape (Fig. 2.d). Alteration of cell morphology in Ad5/mT infected cells was therefore dependent on mT expression and not due to expression of other vector encoded proteins.

Using immunofluorescence, the earliest time for detectable polyoma mT

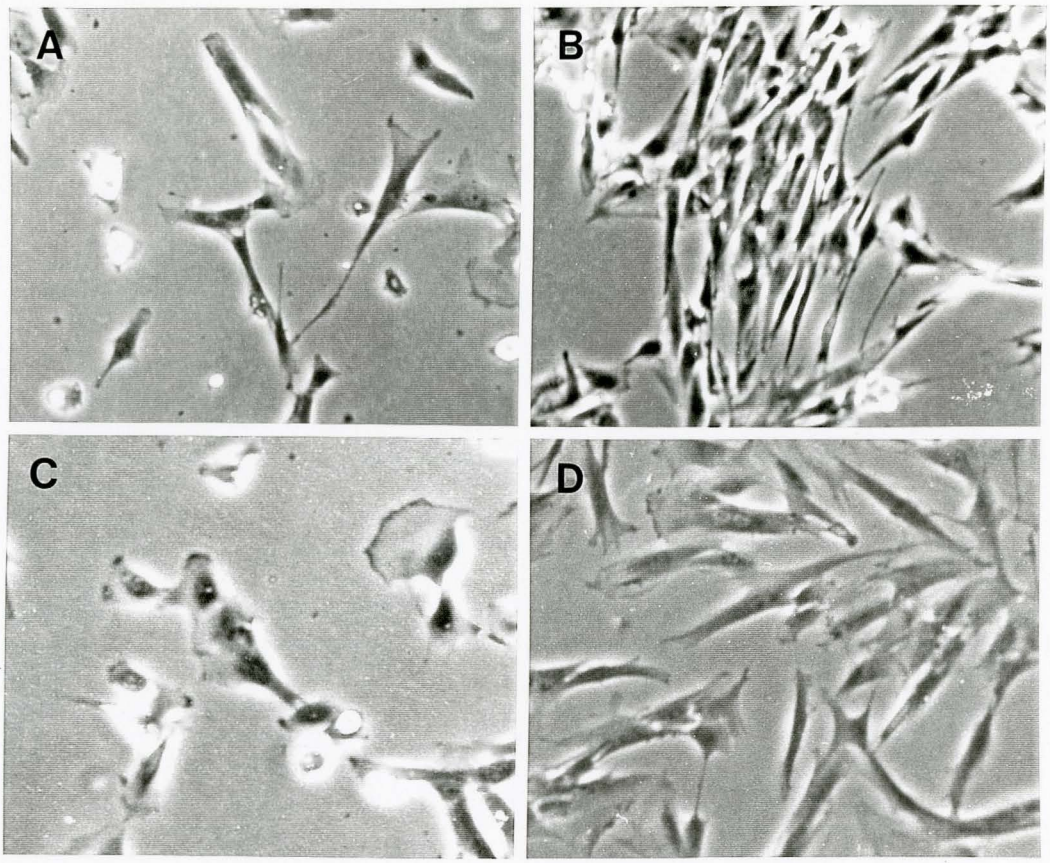

FIG. 2. Cell morphology of Ad5/mT or Ad5/Gp infected MRC5 cells at 40 and 50 hours. MRC5 cells were grown to 40% confluency and infected with same amounts ($5.6x10^8$ plaque forming units [pfu]) of either Ad5/mT or Ad5/Gp virus. Shown are images obtained by phase contrast microscopy. A) MRC5 cells infected with Ad5/mT and B) with Ad5/Gp at 40 hours. C) MRC5 cells infected with Ad5/mT and D) infected with Ad/Gp at 50 hours.

expression was also 40 hours post infection (Fig. 3.a). At this time point the ~50% of cells beginning to change shape also express detectable amounts of mT. Antigen-staining was confined to intracellular structures in the perinuclear area. Only occasionally were cells observed with weak plasma membrane staining. In the same cell, phalloidin staining of actin filaments revealed that first alterations in cell morphology correlated with expression and perinuclear localization of mT at 40 hours (Fig. 3.b). By comparision, in Ad5/Gp infected MRC5 cells, 40 hours post infection the rabies G-protein was prominent in intracellular membranes (Fig. 3.c), but phalloidin/actin staining (Fig. 3.d) showed no alterations in the cytoskeleton or cell morphology consistent with the results obtained by phase contrast microscopy (Fig. 2.b).

At 50 hours post Ad5/mT infection, most of mT antigen is still located in the perinuclear area (Fig. 3.e). By this time phalloidin staining of actin in the same cell revealed total disassembly of the actin cytoskeleton (Fig. 3.f) consistent with the partial loss of cell adherence obvious in figure 2.c. In contrast Ad5/Gp infected cells still showed no alteration in cell morphology (Fig. 3.g, h), despite staining around perinuclear membranes, in structures throughout the cytoplasm and at the plasma membrane (Fig. 3.g).

72 hours after Ad5/mT infection, the cells exhibit a rounded cell shape, disassembly of the actin cytoskeleton (Fig. 4.b), mT distribution throughout the cell, and consistent areas of plasma membrane staining (Fig. 4.a) were observed. At this time, Ad5/Gp infected cells exhibited high levels of expression of rabies G-protein throughout the cells (Fig. 4.c), with only slight

FIG. 3. Immunofluorescence localization of mT, rabies G-protein (Gp) and actin in infected MRC5 cells by confocal microscopy. MRC5 cells were grown to 40% confluency and infected with $5.6x10^8$ pfu of either Ad5/mT or Ad5/Gp and prepared for immunofluorescence as described in section 2.4. Cells were costained for mT and actin or Gp and actin respectively. A) mT staining and B) actin staining 40 hours after Ad5/mT infection. C) Gp specific and D) actin specific staining 40 hours after Ad5/Gp infection. E) MT staining, F) actin staining at 50 hours post Ad5/mT infection. G) Gp staining, H) actin staining of cells at 50 hours post Ad5/Gp infection. Note: at 40 hours roughly 1/2 of the cells are not yet producing detectable mT or Gp. Expression of the proteins is obvious in all cells at 50 hours. Bars, 25 μm.

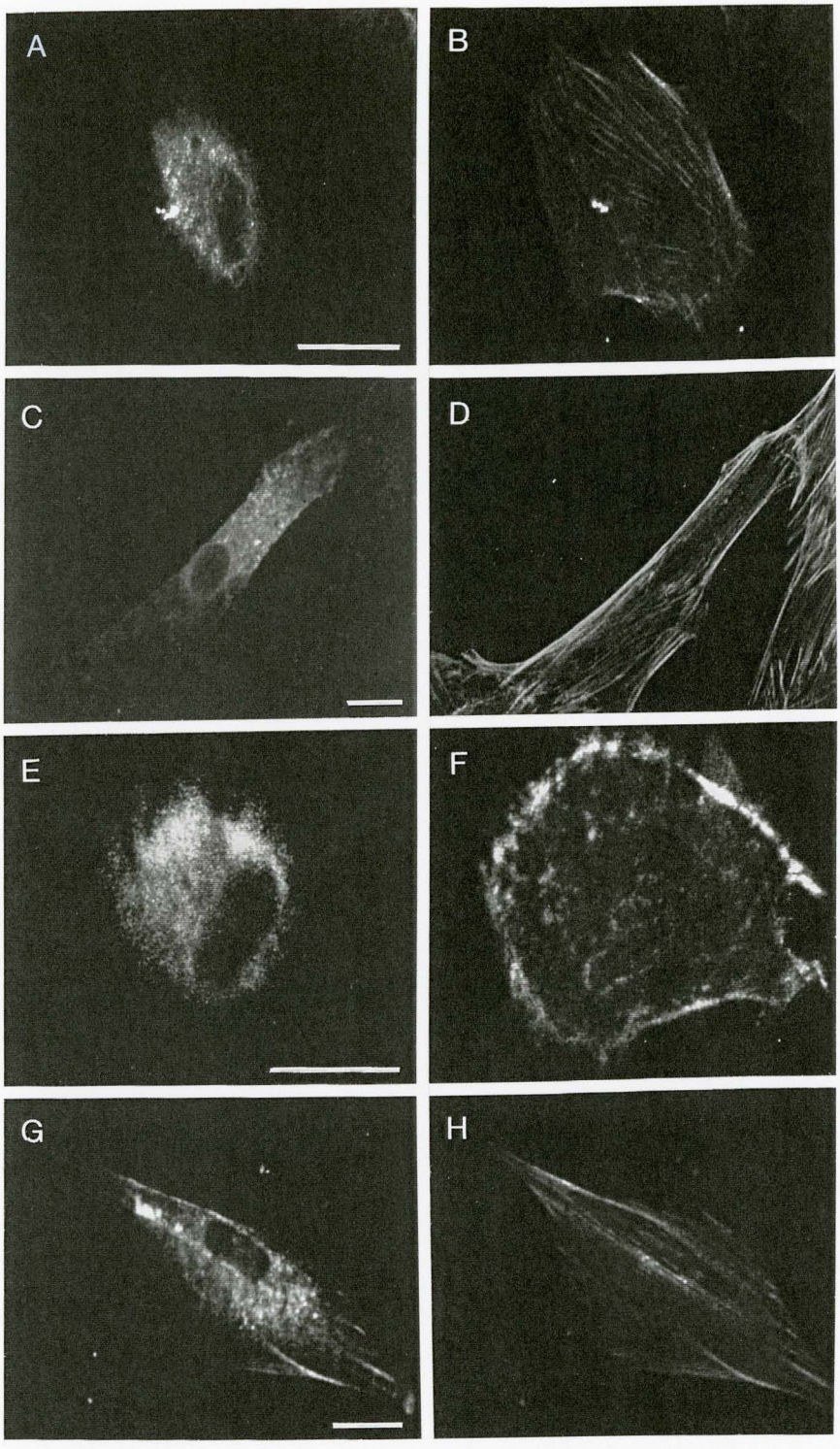
A
B
C
D
E
F
G
H

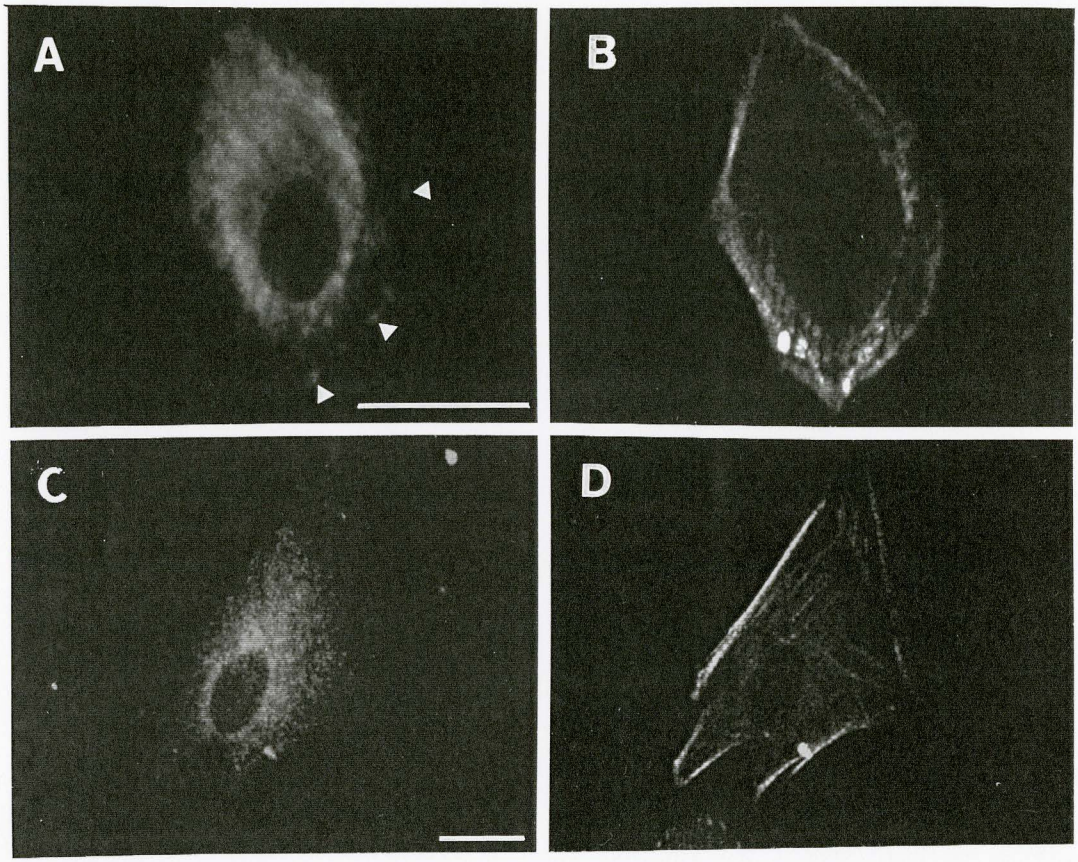

FIG. 4. Immunofluorescence localization of mT, rabies G-protein (Gp) and actin in infected MRC5 cells by confocal microscopy late in infection. MRC5 cells were grown to 40% confluency, infected with Ad5/mT or Ad5/Gp, and processed as described in section 2.4. Cells were costained for mT and actin or Gp and actin respectively. A) mT staining (arrowheads indicate plasma membrane staining) and B) actin staining of Ad5/mT infected cells at 72 hours. C) Gp staining and D) actin staining of Ad5/Gp infected cells at 72 hours.

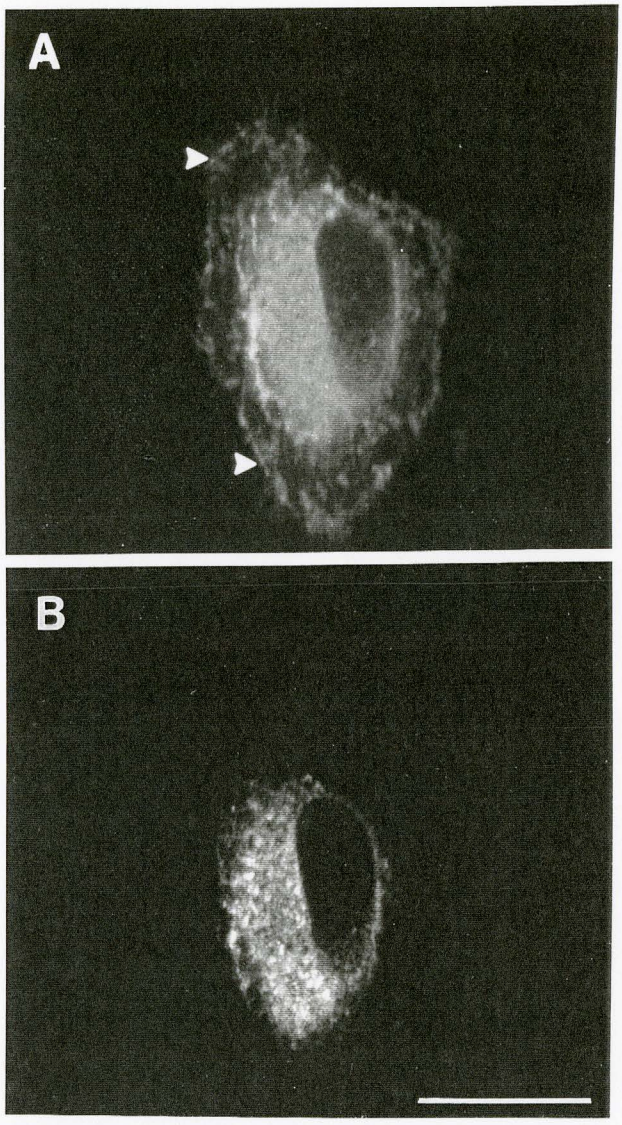

FIG. 5. Immunofluorescence staining of rabies G-protein and mT-antigen in Ad5/mT and Ad5/Gp coinfected MRC5 cells at 50 hours. Cells were coinfected with equal amounts of Ad5/mT and Ad5/Gp virus and processed as described in section 2.4. Representative image overlays of staining A) specific for Gp (arrowheads indicate staining of plasma membrane) and B) specific for mT.

alterations in the actin cytoskeleton and cell morphology (Fig. 4.d). The change in cell morphology is probably due to the extended period of growth in media containing only 2% horse serum (as described in section 2.4) because uninfected MRC5 cells grown under the same conditions exhibited the same slight changes in morphology (data not shown). Therefore the experimental conditions used here are not suitable for examining subcellular changes that occur more than 70 hours after infection.

In MRC5 cells coinfected with Ad5/mT and Ad5/Gp, mT was still located around the perinuclear area 50 hours after infection (Fig. 5.b). In contrast the rabies G-protein was detected in both perinuclear and at the plasma membrane (Fig. 5.a). As expected the morphology of coinfected cells was characteristic for those infected with Ad5/mT.

Our findings regarding the localization of polyoma mT confirm the previous reports of mT antigen in a perinuclear area in transformed or lytically infected cell lines (35,36). However, at early time points (40-50 hours) mT is not localized to the plasma membrane. In addition, cell morphology can be altered by mT at this perinuclear location early in infection. These results suggest that the mT population found at the plasma membrane in previous biochemical analysis (49, 50, 85) and in Ad5/mT infected MRC5 cells later on in the infection is not involved in the subcellular changes that occur at the onset of cell transformation by mT.

3.3 Subcellular compartment of initial polyoma mT localization.

To more precisely localize polyoma mT in fibroblasts, we used several antibodies against markers of specific membrane compartments. These markers were analyzed in normal MRC5 cells, and selected markers showing compartment specificity were also used in cells 40 hours post Ad5/mT infection. Cells expressing mT were identified by the onset of morphology changes. Only cells early in infection with morphology changes characteristic for perinuclear localized mT were examined. In addition, to ensure that a productive infection with Ad5/mT had occured one coverslip from the same dish was stained for mT and examined by confocal microscopy.

Cells were grown to ~ 40% confluence and then processed as described in 2.4. Table II gives an overview of the antibodies used, the compartments identified in MRC5 cells, and indicate whether or not changes in the staining pattern occured after Ad5/mT cell infection. Antibodies against specific compartments marked with an asterisk were used to further investigate mT antigen subcellular localization. Typical representative images from confocal laser scanning microscopy are presented in figures 6 and 7.

To identify the endoplasmic reticulum in MRC5 cells we examined antibodies to the α-subunit (SRα [polyclonal rabbit], SRα [monoclonal mouse]) and the β-subunit (SRβ) of the signal recognition particle receptor, the α-subunit (SSRα) and β-subunit (SSRβ) of "signal sequence receptor", oligosaccharyl transferase and calnexin. SSRα and monoclonal SRα

Table II. Antibodies used in immunofluorescence studies against markers of the Endoplasmic reticulum (ER), Golgi apparatus and intermediate compartment.

Marker	MRC5 uninfected	MRC5 Ad5/mT infected
Endoplasmic reticulum (ER):		
SSRα	no staining	n/a
SSRβ	weak ER specific staining	no change visible
SRα (polyclonal)	high background	no change visible
SRα (monoclonal)	no staining	n/a
SRβ	non-specific staining	no change visible
oligosaccharyl transferase	non-specific staining	no change visible
calnexin	high background	no change visible
calnexin (affinity purified)*	ER specific staining	no change visible
Golgi apparatus:		
β-COP*	Golgi apparatus specific staining	no change visible
mannosidase II	Golgi apparatus specific staining	no change visible
Intermediate compartment:		
ERGIC-p53* (mouse monoclonal)	Staining characteristic for ERGIC-53	no change visible

Table II. Antibodies used against markers of the trans-Golgi network (TGN), late endosomes, tubular endosomes and mT antigen.

Marker	MRC5 uninfected	MRC5 Ad5/mT infected
Trans-Golgi network (TGN):		
TGN-38	non-specific staining	no change visible
Late endosomes & TGN:		
CI-MPR* (mannose-6-ph-receptor)	specific staining	no change visible
Secondary lysosomes & late endosomes:		
LE*	specific staining	at later times staining around perinuclear area and plasma membrane

Uninfected or Ad5/mT infected MRC5 cells were grown to ~ 40% confluence and then treated as described in section 2.4. All primary antibodies are polyclonal rabbit antisera unless otherwise stated. Secondary antibodies were conjugated with FITC. Marker stainings of uninfected and infected cells were analyzed by indirect immunofluorescence with a confocal laser microscope. Antibodies marked with an asterisk were used in further studies.

antibodies exhibited no binding in normal MRC5 cells. Antiserum against SRβ showed non-specific cell staining, and polyclonal antibodies to SRα a high background and nuclear staining was visible. Nuclear and non-specific staining of these antibodies in MRC5 cells is likely to be caused by crossreactivity of the antiserum. The only antiserum of the signal recognition particle receptor or signal sequence receptor series which gave specific ER staining was SSRβ. Staining of an intracellular membrane network concentrated around the perinuclear area, but at the same time also extended throughout the cytoplasm characteristic of the ER was visible (41). There was no change in the staining pattern after Ad5/mT infection. Polyclonal antisera against the endoplasmic reticulum markers oligosaccharyl transferase or calnexin resulted in high background and non-specific staining. However, when immunoaffinity purified polyclonal anti-calnexin antibodies were used, excellent staining of the ER was evident (Fig. 6.a). The antibodies stained a perinuclear region and structures throughout the cytoplasm, resembling ER specific staining in other cells (41, 37), but distinct from subcellular mT localization (Fig. 3.a), suggesting that mT is not found in the ER. Infection of the cells with Ad5/mT did not produce visible changes in ER structure or morphology (Fig. 6.b), confirming the results observed with SSRβ antibodies.

The Golgi apparatus, identified by indirect immunofluorescence as a network of stacked tubular membranes usually located on one side next to the nucleus (89), plays a key role in protein processing. Data obtained with

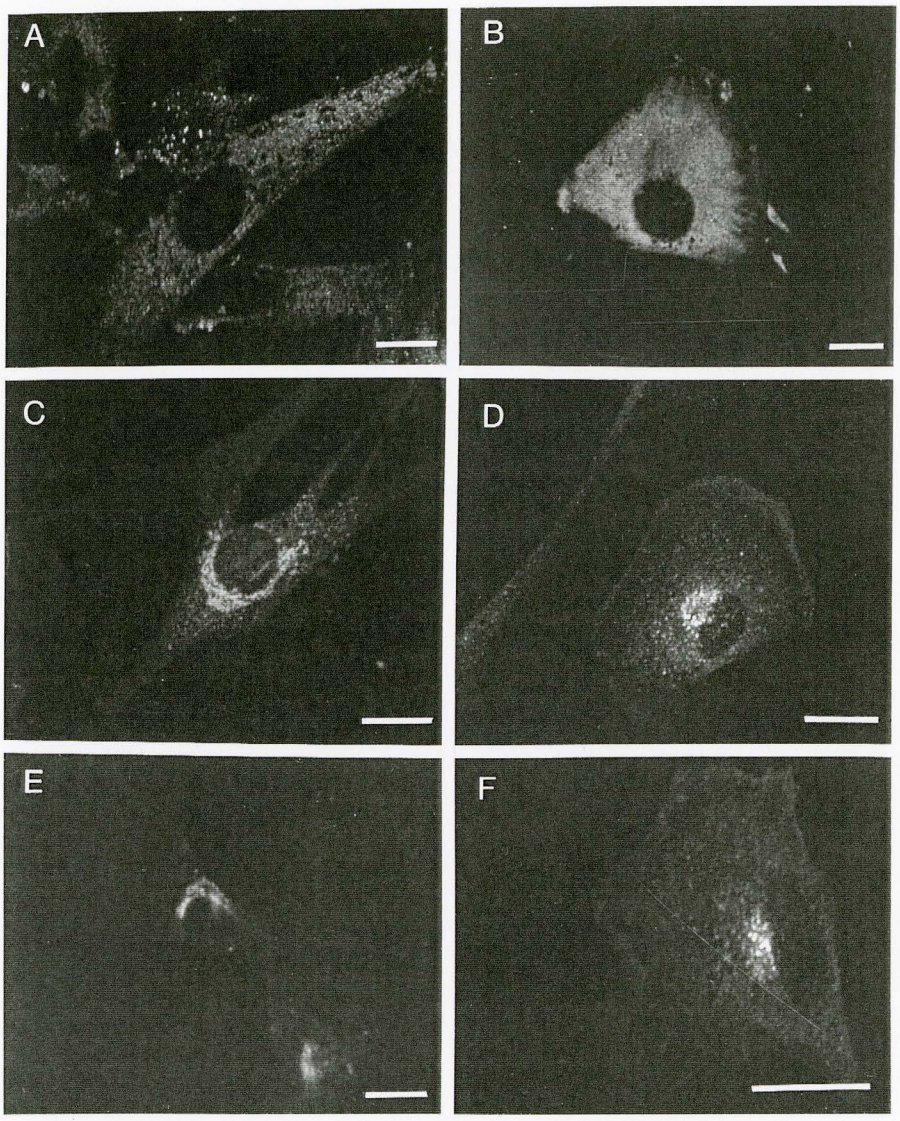

FIG. 6. Fluorescent immunolocalization of different subcellular compartment markers in uninfected and Ad5/mT infected MRC5 cells. Cells were prepared as described in section 2.4. Staining pattern specific A) for calnexin (ER-marker), C) for β-COP (Golgi-marker) and E) for CI-MPR (Late endosome and TGN marker) in uninfected cells. Staining for B) calnexin, D) β-COP and F) CI-MPR in Ad5/mT infected cells at 40 hours after infection.

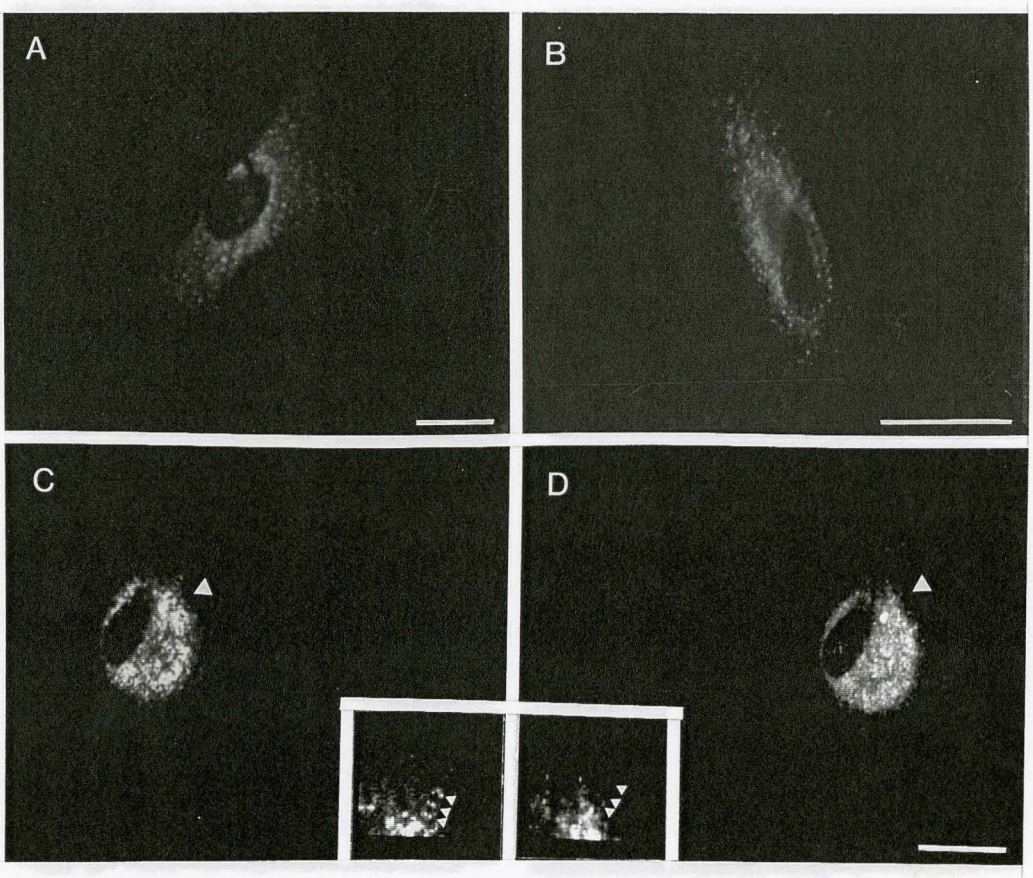

FIG. 7. Fluorescent immunolocalization of ER-Golgi intermediate compartment marker ERGIC-53 in uninfected and Ad5/mT infected MRC5 cells and double immunofluorescence localization of ERGIC-53 and mT in Ad5/mT infected MRC5 cells. Cells were prepared and infected as described in section 2.4. Staining pattern specific for ERGIC-53 (intermediate compartment marker) A) in uninfected cells and B) in Ad5/mT infected cells at 40 hours after infection. C) Staining for ERGIC-53 and D) staining for mT in ERGIC-53/mT costain in cells at 40 hours after Ad5/mT infection. Insets in (C) and (D) are enlargements of the areas indicated by arrowheads and show partial non overlap (arrowheads in insets) of mT and ERGIC-53 staining pattern.

antibodies against the Golgi markers β-COP ([coatomer associated protein], Fig. 6.c/Tab. II) and mannosidase II (Tab. II) resulted in prominent staining of the Golgi apparatus in uninfected MRC5 cells which coincided with the staining pattern in normal rat kidney (NRK) cells as described above (89). This Golgi-specific staining pattern also differed from the mT compartment. β-COP is a component of the non-clathrin-coated vesicles and is present in a multisubunit protein complex named "coatomer" (48). This complex plays an essential role in the transport between the ER and the Golgi apparatus and between early Golgi compartments (48, 107). Infection of fibroblasts with the Ad5/mT vector did not have any impact on Golgi apparatus configuration and subsequently no change in the staining pattern was obvious (Fig. 6.d/Tab. II for β-COP and in Tab. II for mannosidase II).

Late endosomes and the trans-Golgi network can be identified with antibodies against the cation-independent mannose-6-phosphate receptor (CI-MPR), a component of the protein sorting mechanism which mediates the transport of lysosomal enzymes marked with mannose-6-phosphate (38). Staining with polyclonal antibodies against CI-MPR revealed the expected trans-Golgi pattern (38), consisting of prominent staining of accumulated vesicles close to the nucleus, for uninfected (Tab. II/Fig. 6.e) and Ad5/mT infected cells (Tab. II/Fig. 6.f), with no overlap with mT. Therefore mT is not located in late endosomes or in the trans-Golgi network. In addition, the compartments appear not to be targets of mT during cell transformation.

In contrast, staining of the recently defined ER-Golgi intermediate compartment (ERGIC) using monoclonal antiserum to ERGIC-53 (39, 40, 41, 42) in either uninfected or Ad5/mT infected MRC5 cells showed a perinuclear staining pattern in MRC5 cells very similar to mT (Tab. II/Fig. 7.a and b). The ERGIC-53 pattern in MRC5 cells was also consistent with previous results obtained in Vero cells (41).

To further investigate the relationship of the intermediate compartment and mT distribution at the onset of cell transformation, mT and ERGIC-53 double immunofluorescence was performed. MRC5 cells were grown and infected as described above. All results of double label immunofluorescence have been verified and controlled with secondary antibodies conjugated to different fluorescent dyes (as described in 2.1 and 2.4). In addition, the results were confirmed by using either affinity purified polyclonal rabbit anti-mT antibody or monoclonal rat anti-mT antibodies (721/722). Representative results for ERGIC-53/mT costains are shown in figure 7.c and d.

Immunofluorescence analysis of ERGIC-53/mT confirmed earlier results suggesting a perinuclear localization of both proteins at 40 hours post infection (Fig. 7.c and d). However, as shown by the insets (Fig. 7.c and d, area indicated by arrowheads) mT and ERGIC-53 staining of perinuclear areas did partly non overlap (indicated by arrowheads in insets). Furthermore, in a number of infected cells the mT specific staining extended further into the cytoplasm than did ERGIC-53 staining (data not shown).

3.4 The mT compartment is Brefeldin A resistant.

To address the possibility that the mT distribution partially overlaps that of the intermediate compartment identified by ERGIC-53 we examined the sensitivity of both compartments to BFA. The fungal metabolite BFA is widely used in the field of membrane trafficking and organelle structure research, and has provided important insights into the dynamic organization of the ER/Golgi membrane system (43, 44, 48). In a number of cells, BFA prevents the assembly of COPs coated vesicles, which were until recently only implicated to be essential for membrane traffic from the ER to the Golgi apparatus (44, 48). However, previous results suggest that COPs coated vesicles also play an important role in retrograde vesicle transfer from the Golgi to the ER (107). Whether anterograde and retrograde vesicles are coated with two different sets of COPs has still to be determined (107). Because BFA prevents the assembly of COPs onto coated vesicles, newly synthesized proteins cannot exit the ER (44, 48). The recent results implicating COPs coated vesicles also in retrograde vesicle transfer offer an possible explanation for the second phenomena namely that BFA treatment of cells disrupts the structure of the Golgi apparatus and causes retrograde (tubular) transport from the Golgi to the ER (44, 48). This transport was thought to occur through uncoated tubules (44, 48). In addition, previous findings suggest that the retrograde moving vesicles that lack COPs are no longer able to bud off the Golgi apparatus and therefore whole Golgi tubules are integrated into the ER (107). The effects of BFA treatment on the trans-Golgi network (TGN) are less clear (43, 46, 45, 38).

While some cells exhibit morphology changes, e.g. induction of an extensively fused network of membranes derived from the TGN and early endosomes (43,46), others observe a collapse of the majority of the TGN around the microtubule organizing center (45, 38). However, it is unanimously agreed that BFA treatment does not cause retrograde transport from the TGN to the ER, and endocytic traffic from the cell surface to the TGN is unaffected (44). The influence of BFA on the ERGIC-53 containing intermediate compartment is cell type specific. In some cell systems, the compartment appears resistant to the drug (48); while in others vesicular redistribution over the entire cytoplasm is observed (47).

To investigate whether perinuclear localized mT and the intermediate compartment marked by ERGIC-53 were similarly or differentially sensitive to BFA, MRC5 cells were infected for 40 hrs with Ad5/mT, treated with BFA and then stained with antibodies against mT, ERGIC-53 and β-COP. Corresponding negative controls without BFA were prepared as usual. Representative confocal laser scanning micrographs are shown in figure 8.

BFA treatment did not affect mT staining (Fig. 8.a and 3.a) as the molecule is still located in the perinuclear region. However, the staining pattern of ERGIC-53 showed dramatic changes after exposure to BFA. The perinuclear distribution of ERGIC-53 (Fig. 7.a, b, c) was converted to large dots spread over most of the cytoplasm (Fig. 8.b). As a positive control for the expected effects of BFA on the cells, fibroblasts were also stained for β-COP. As expected BFA

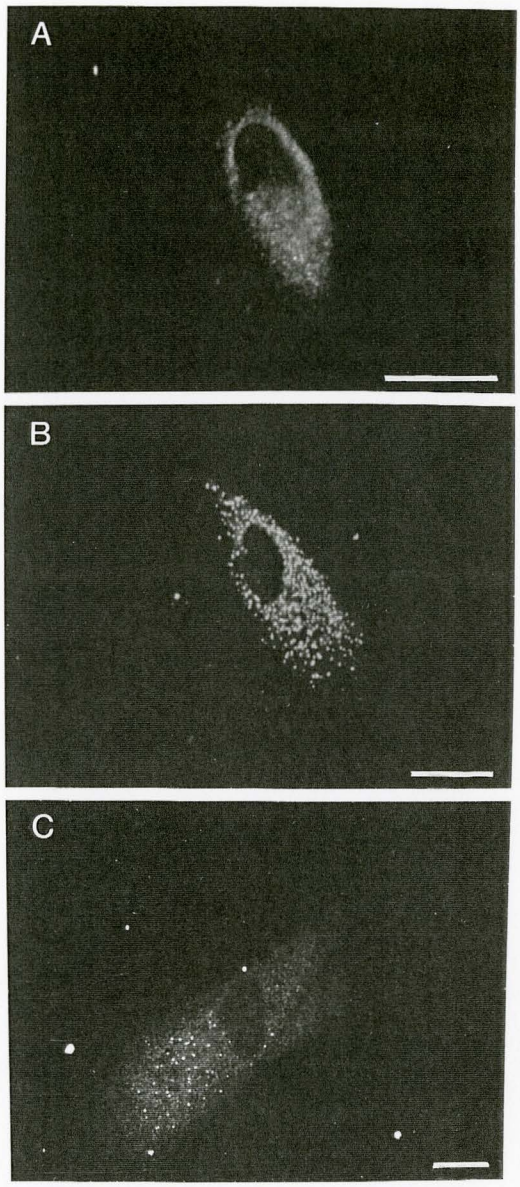

FIG. 8. Immunofluorescence localization of mT, ERGIC-53 and β-COP after brefeldin A treatment of Ad5/mT infected MRC5 cells. Cells were infected as in Fig. 11. Before further processing, cells were incubated for 45 min with 5μg/ml BFA, then fixed and prepared as described in section 2.4. Staining pattern specific for mT (A), ERGIC-53 (B) and β-COP as BFA positive control (C) are shown.

treatment of infected cells disrupted the Golgi structure and β-COP was widely dispersed throughout the cytoplasm (Fig. 8.c). The positive control was therefore consistent with results obtained earlier in normal rat kidney (NRK) cells (89).

Therefore the subcellular structure that contains polyoma mT antigen is BFA resistant, and does not coincide with the intermediate compartment marked by ERGIC-53.

3.5 Identification of a mT target

The 100 kDa protein LE is found primarily in secondary lysozomes and late endosomes (personal communication J.J.M. Bergeron). In uninfected cells the majority of the protein was distributed in a typical punctate pattern throughout the cytoplasm, with small amounts in plasma membranes (Fig. 9.a, b). Although mT clearly does not co-localize with LE, staining with tubular endosomal antibody against the marker protein LE revealed alterations in morphology after cell infection. At 40 hours post infection the pattern was not radically different from that observed in uninfected cells (Fig. 9.c) even though morphology is clearly altered (Fig. 9.d). However, by 50 hours post infection staining for LE in Ad5/mT infected MRC5 cells was more concentrated around the nucleus (Tab. III/Fig. 9.e, f). In addition, prominent plasma membrane staining (indicated in figure 9.e by arrows) confirmed that this subcellular compartment is dramatically reorganized 50 hours post infection with Ad5/mT.

To further investigate secondary lysosomes and late endosomes identified by the protein marker LE and their relationship with mT subcellular localization, double immunofluorescence was performed. For LE/mT double immuno-fluorescence, polyclonal rabbit LE antiserum and monoclonal rat anti-mT antibodies 721/722 were used. In LE/mT costains, both proteins exhibited perinuclear staining; however, LE staining extended further into the cytoplasm and was also very prominent at plasma membranes at 50 hours

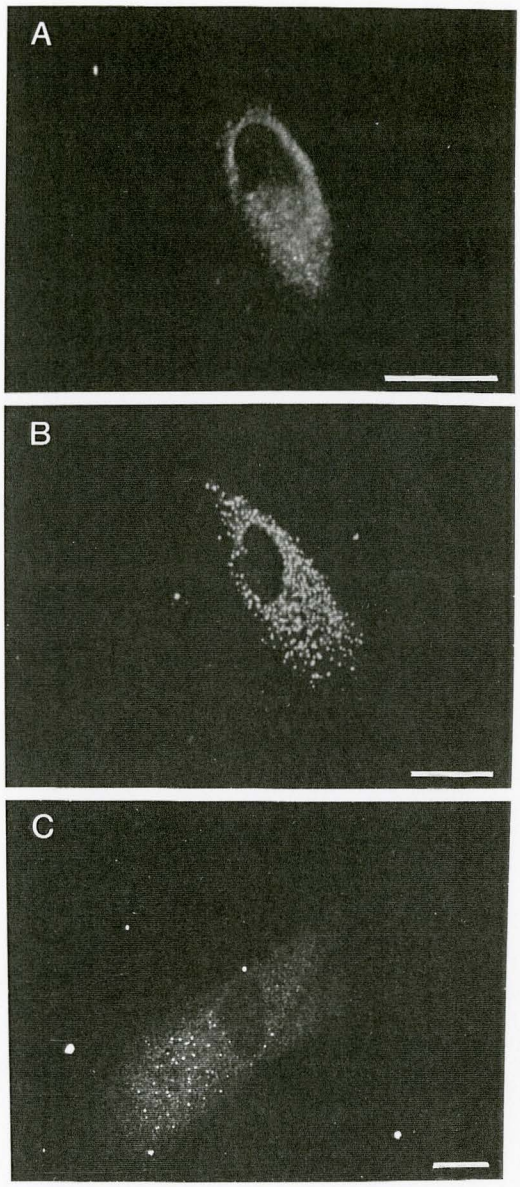

FIG. 8. Immunofluorescence localization of mT, ERGIC-53 and β-COP after brefeldin A treatment of Ad5/mT infected MRC5 cells. Cells were infected as in Fig. 11. Before further processing, cells were incubated for 45 min with 5μg/ml BFA, then fixed and prepared as described in section 2.4. Staining pattern specific for mT (A), ERGIC-53 (B) and β-COP as BFA positive control (C) are shown.

after Ad5/mT infection (data not shown), confirming above results (Fig. 9). The results suggested therefore, that mT distribution does not coincide with the tubular endosome population represented by the LE marker, but that the distribution of LE is altered as cellular morphology is rearranged by mT.

3.6 Early changes in cytoskeletal components induced by mT

Our initial examination of morphology changes induced by mT in 293 N3S and Rat-2 cells suggested that at least part of the actin cytoskeleton is associated with mT complexes (3). To examine these changes in more detail and to examine other elements of the contractile cytoskeleton, we assessed the interaction of polyoma mT at the perinuclear location with components of the cytoskeleton in Ad5/mT infected MRC5 cells at the onset of the morphology changes. The cytoskeleton is formed by three different classes of filamentous assemblies: microfilaments, intermediate filaments and microtubules. Together they define cell shape and are responsible for vesicle transport, shape changes and cell migration. As typical representatives of these classes in fibroblasts, we selected the proteins actin (microfilaments), vimentin (intermediate filaments) and β-tubulin (microtubules).

MRC5 cells were infected with Ad5/mT virus, incubated for 40 hours, and processed in the usual manner with either a fluorescent phalloidin conjugate (staining filamentous actin) (74), or monoclonal antibodies against vimentin, anti-β-tubulin, or polyclonal immuno-purified anti-mT antibodies. In addition, a set of slides was prepared by permeabilizing cells before fixation with a buffer that extracts soluble proteins to determine if any of the cytoskeletal components were disassembled and therefore extractable. As controls uninfected fibroblasts were treated similarly and stained for the same markers. In addition, actin staining was examined in Ad5/Gp infected cells after 50 hours.

Characteristic images obtained by confocal laser scanning microscopy are presented in figure 10 and figure 11. In uninfected cells treated with the cytoskeletal extraction buffer, markers for vimentin (Fig. 10.a), actin (Fig. 10.b) and β-tubulin (Fig. 10.c) show an intact and widespread filamentous network. As expected at the onset of the morphology changes induced by mT expression, all three cytoskeletal markers showed some alterations in normally prepared/fixed cells (Fig. 11.a, c, e, g). The image in Fig. 11.c shows altered cell morphology, rearrangement of the actin skeleton, and the first stage of actin depolymerization (also seen in figure 3.b). Because phalloidin binds to actin filaments, but not to actin monomers, phalloidin fluorescence is a good measure of the amount of filamentous actin in cells (74). Vimentin filaments started to collapse at the the outer cell border but remained a largely intact filament network (Fig. 11.e). This process was even more obvious in β-tubulin stained cells (Fig. 11.g).

In MRC5 cells treated with the cytoskeletal extraction buffer 40 hours after Ad5/mT infection, only a small fraction of the mT staining remained in the cells presumably indicating that this mT was partially bound to the cytoskeleton at the perinuclear location after extraction of soluble cellular proteins. Visual inspection of the slides suggests only ~ 30% of the expressed mT remained bound to detergent insoluble structures (Fig. 11.b). However, all of the filamentous actin was extracted with the low salt detergent containing buffer (figure 11.d). In contrast, components of the vimentin network

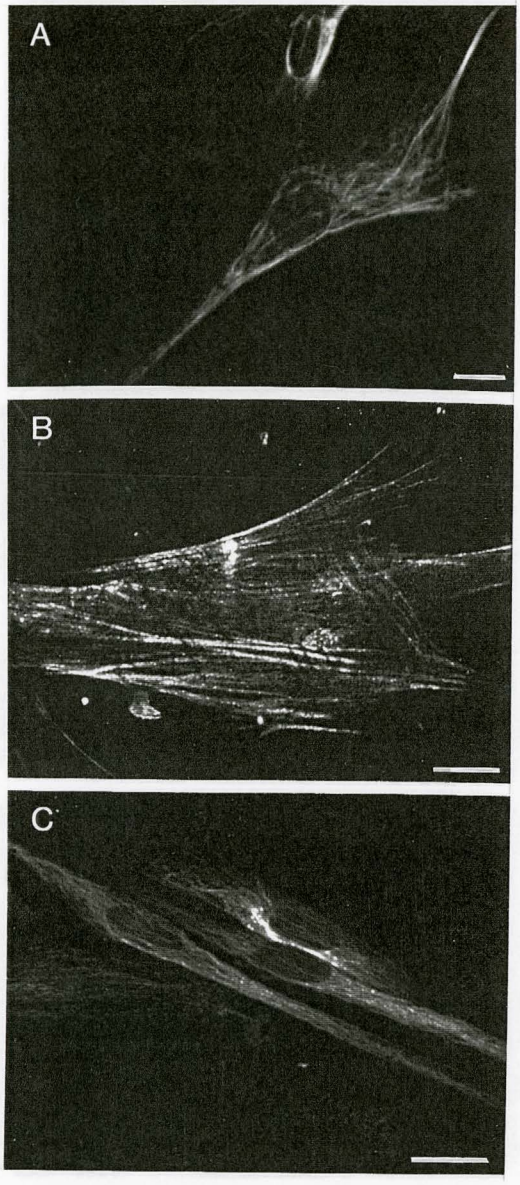

FIG. 10. Fluorescent immunolocalization of the cytoskeletal markers actin, vimentin and β-tubulin in normal MRC5 cells after extraction of soluble proteins. Cells were grown to ~ 40% confluency and treated with the cytoskeleton stabilizing buffer. Soluble proteins were extracted, the remaining cytoskeletal elements were fixed and treated as described in section 2.4. Staining pattern specific for phalloidin binding to vimentin filaments (A), and for actin (B) and β-tubulin (C).

FIG. 11. Immunofluorescent localization of mT (A, B), actin (C, D), vimentin ((E, F) and β-tubulin (G, H) in Ad5/mT infected MRC5 cells at 40 hours. Cells were infected with Ad5/mT as described in section 2.4. Half of the cells were fixed, permeabilized and stained as usual (A, C, E, G). The other cells were first treated with the cytoskeletal stabilizing buffer, then soluble proteins were extracted; the cells were fixed and then treated as usual (B, D, F, H). Actin staining was not visible after extraction of soluble cell proteins.

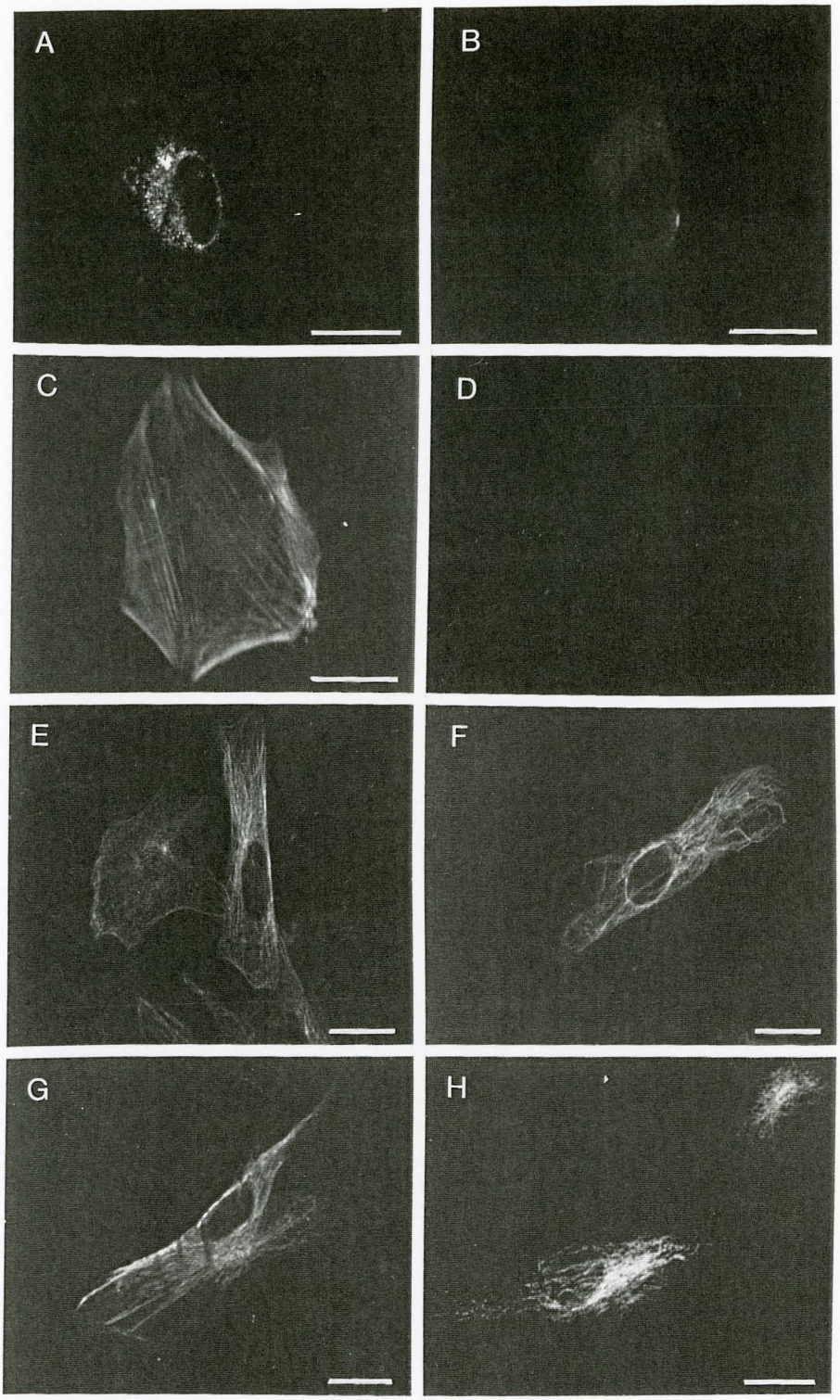
A
B
C
D
E
F
G
H

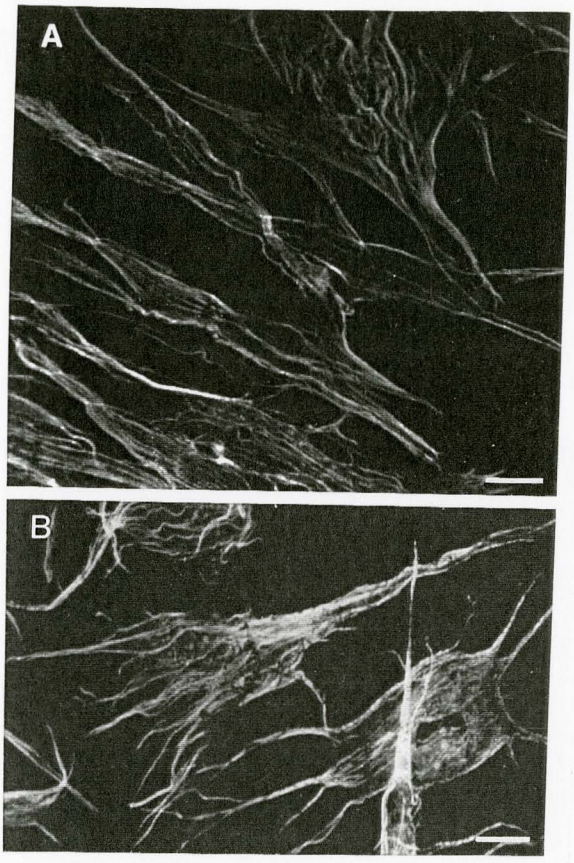

FIG. 12. Immunofluorescence localization of actin in Ad5/Gp infected MRC5 cells at 50 hours (A, B). Cells were infected with Ad5/Gp as described in section 2.4, treated with the cytoskeletal stabilizing buffer, and soluble proteins were extracted. The cells were then fixed and treated as usual.

were not extractable (Fig. 11.f) and only slight differences in β-tubulin staining were observed (Fig. 11.h). This result confirmed our earlier observation, that actin cytoskeleton appears to be an early target of mT (3). Furthermore it suggests that after actin depolymerization remaining mT is associated with other detergent insoluble structures. At the onset of morphology changes these structures could be vimentin or β-tubulin.

In an assay performed at 50 hours post infection in Ad5/Gp infected MRC5 control cells, the actin cytoskeleton remained intact (Fig. 12.a and b). As indicated in Fig. 3.g presented in section 3.2, the rabies-Gp protein is clearly overexpressed at 50 hours post Ad5/Gp infection. Therefore this finding confirms our earlier results presented in section 3.2 that depolymerization of filamentous actin depends on mT expression and is not due to expression of other Ad5-vector encoded proteins.

In MRC5 cells prepared using our standard procedure, incubation of the cells for more than 50 hours after infection resulted in alterations in all three filament markers. Whereas the remaining actin staining was in close proximity of the plasma membrane (Fig. 4.b), vimentin and β-tubulin staining were concentrated in a structure resembling the microtubule organizing center (data not shown).

These data support an interaction of perinuclear located mT with distinct cytoskeleton components. In addition, it raises the possibility that mT might influence one primary cytoskeletal target which then causes other cytokeletal

components to alter. Of the three cytoskeleton filaments assessed here, the actin cytoskeleton is the primary target of mT during early alterations in cell morphology.

Other components of the fibroblast cytoskeleton, which were tested include tropomyosin, vinculin and the spectrin homolog fodrin. Indirect immunofluorescence experiments with antibodies to tropomyosin indicated a rearrangement in Ad5/mT infected MRC5 cells similar to actin (data not shown); antisera to vinculin and fodrin did not give conclusive staining patterns and were therefore not tested further.

3.7 Colocalization of known mT binding proteins involved in the signal transduction pathway with mT in perinuclear structures.

The finding that mT is localized to the perinuclear area during the initial alterations in cell morphology raises the question as to whether mT is also able to stimulate mitogenesis from this location. To test this, we looked for colocalization of several proteins involved in the putative mT-signal transduction complex at 40 hours post infection in cells in which morphology changes were just beginning.

The proteins investigated were PP2A, PI3-K, two different 14-3-3 protein family isomers, pp60$^{c\text{-}src}$ and Shc. MRC5 cells were grown to ~ 40% confluency, infected with either Ad5/mT, Ad5/c-src or coinfected with both viruses and prepared for immunofluorescence as in 2.4. The results are summarized in table III. Antibodies used against PP2A, different domains of PI3-K and the zeta or epsilon isoform of the 14-3-3 protein family did not give informative staining patterns and were therefore not further investigated. Representative images from confocal laser scanning microscopy for pp60$^{c\text{-}src}$ and Shc are shown in figures 13 and 14.

Mouse monoclonal antibody to pp60$^{c\text{-}src}$ revealed weak perinuclear membrane staining in uninfected and Ad5/mT infected MRC5 cells. However, the expression of pp60$^{c\text{-}src}$ in these cells was too low to draw any definitive conclusions. Therefore an Ad5/c-src virus was used to increase expression of pp60$^{c\text{-}src}$. 40 hours after Ad5/c-src infection most staining of pp60$^{c\text{-}src}$ was around perinuclear membranes similar to mT staining in

Table III. Antibodies used against proteins known to interact with mT antigen and their staining pattern in uninfected and infected MRC5 cells.

Marker	MRC5 uninfected	MRC5 Ad5/mT infected
PP2A	non-specific nuclear membrane and inner nuclear area staining	no change visible
PI3-K:		
SH2-domain (p85)	non-specific staining	no change visible
SH3-domain (p85)	non-specific staining	no change visible
full-length PI3-K	Binding of cytoskeletal components	no change visible
14-3-3 family:		
zeta ζ isoform	large dots over the entire cytoplasm	no change visible
&		
epsilon ε isoform	large dots over the entire cytoplasm	no change visible
pp60$^{c\text{-}src}$	weak perinuclear staining	no change visible
pp60$^{c\text{-}src}$* in Ad5/c-src infected MRC5 cells:	perinuclear and plasma membrane staining	no change visible
Shc*	cytoplasmic staining	perinuclear and light cytoplasmic staining

Uninfected or Ad5/mT infected MRC5 cells after 40 hours grown to 40% confluence and then treated as described under 2.4. Secondary antibodies were conjugated with FITC. Marker stainings were analyzed by indirect immunofluorescence with a confocal laser microscope. Proteins marked with an asterisk were used in further investigations.

Ad5/mT infected MRC5 cells (figure 13.a, large arrow); however, pp60$^{c\text{-}src}$ was also located at the plasma membrane (small arrows in figure 13.a).

MRC5 cells were also coinfected with Ad5/mT and Ad5/c-src virus strains, incubated for 40 hours and then stained with mouse monoclonal antibody to pp60$^{c\text{-}src}$, affinity purified rabbit polyclonal mT antibody and were further analyzed as described above. In coinfected cells both proteins, mT (Fig. 13.c) and pp60$^{c\text{-}src}$ (13.b), revealed the characteristic pattern of perinuclear staining. However, the area marked by pp60$^{c\text{-}src}$ extended further into the cytoplasm (Fig. 13.b). In contrast with the perinuclear staining patterns observed with other markers (Fig. 6.c, e and Fig. 9.a, b, c) staining was coincident in some structures suggesting that mT and pp60$^{c\text{-}src}$ occupy partly overlapping cellular compartments (Fig. 13.b, c indicated by arrowheads in insets).

Recent reports indicate that mT in transformed Rat-2 cells binds to tyrosine phosphorylated Shc (27). Therefore the location of Shc in normal MRC5 fibroblasts was assessed and compared to Shc localization in infected cells.

As expected for a cytosolic protein, the polyclonal affinity purified anti-Shc antibody revealed protein evenly distributed over the entire cytoplasm in uninfected cells (Fig. 14.a). Significantly, recruitment of Shc protein to the perinuclear mT location was observed in Ad5/mT infected cells (figure 14.b). In some cells not all of the Shc was relocalized as weak cytoplasmic staining was also visible. In addition, in some cells faint staining of the plasma

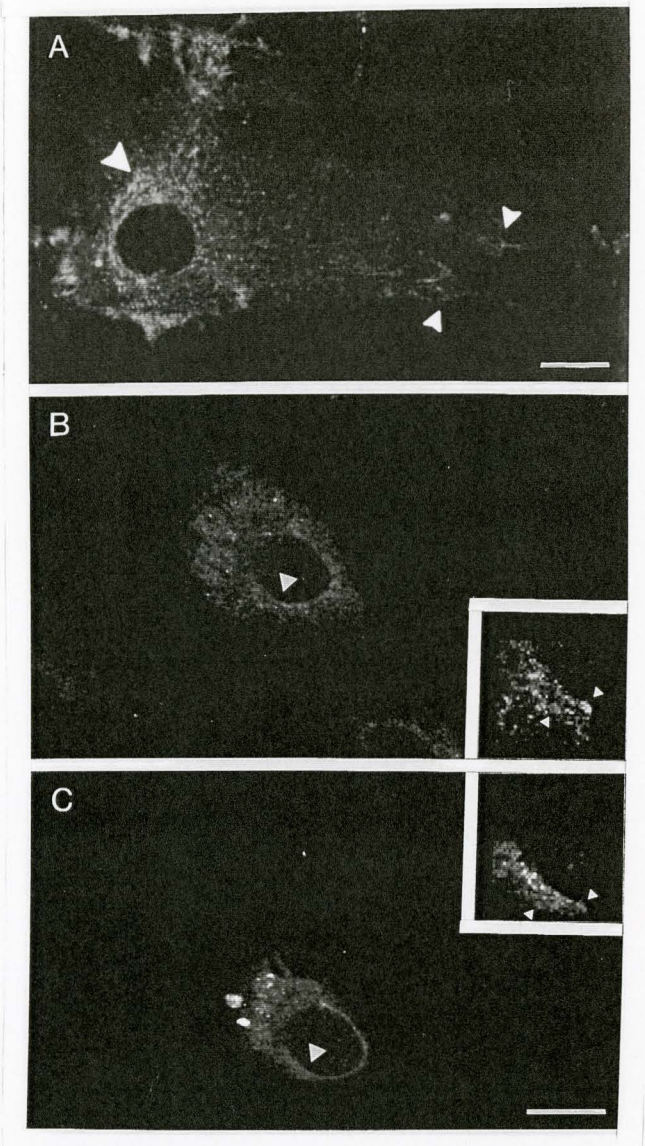

FIG. 13. Polyoma mT-antigen and pp60$^{c\text{-}src}$ immunofluorescence of Ad5/mT infected or Ad5/mT and Ad5/c-src coinfected MRC5 cells at 40 hours. Cells were prepared as described in section 2.4. Staining pattern specific for pp60$^{c\text{-}src}$ in Ad5/c-src infected cells (A); small arrowheads indicate plasma membrane staining and large arrowhead indicates perinuclear staining. Staining pattern specific for pp60$^{c\text{-}src}$ (B) and for mT (C) in Ad5/mT and Ad5/c-src coinfected cells. Insets in (B) and (C) are enlargements of the areas indicated by arrowheads and show partial overlap of pp60$^{c\text{-}src}$ and mT staining pattern (indicated by arrowheads in insets).

FIG. 14. Fluorescence immunolocalization of Shc in uninfected or Ad5/mT infected MRC5 cells, and effects of brefeldin A treatment. Fibroblasts were infected and prepared as in section 2.4. Brefeldin A treated cell samples were incubated with 5μg/ml BFA for 45 min prior to cell fixation. FITC staining of Shc in uninfected cells (A), in Ad5/mT infected cells 40 hour post infection (B), in Shc/mT costains of Ad5/mT infected cells at 40 hours (C) and in Shc/mT costains of Ad5/mT infected cells at 40 hours treated with BFA (E) are shown. Texas red staining of mT in Shc/mT costains of Ad5/mT infected cells at 40 hours (D) and of mT in Shc/mT costains of Ad5/mT infected cells at 40 hours treated with 5μg/ml BFA (F).

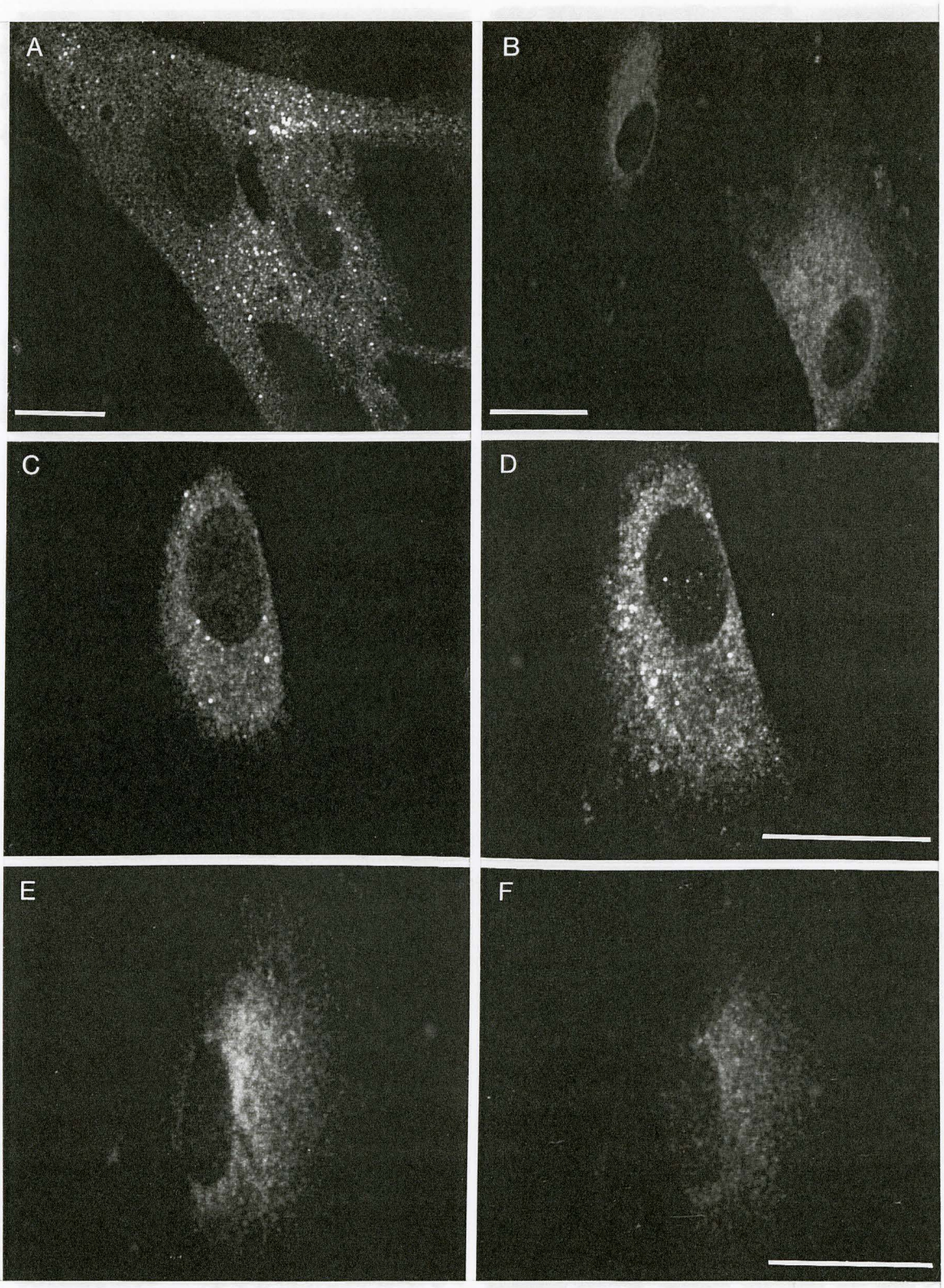
A
B
C
D
E
F

membrane was seen. However, plasma membrane staining was only evident in cells which exhibited more advanced changes in morphology similar to cells in which mT was also detected at the plasma membrane.

In Shc/mT costains, both mT and Shc were seen in perinuclear structures (Fig. 14.c and d). Similar to mT, brefeldin A had no effect on Shc distribution (figure 14.e and f).

Together these results suggest that mT can potentially interact with pp60$^{c\text{-}src}$ and Shc while located in the perinuclear region. Therefore the signals for mitogenesis transduced by proteins like pp60$^{c\text{-}src}$ and Shc may occur at the perinuclear rather the plasma membrane.

3.8 Examination of Shc and mT-antigen distribution in different MRC5 cell fractions.

The results of the immunofluorescence investigations predicted that the difference in Shc subcellular localization after mT infection in MRC5 cells should be detectable by biochemical cell fractionation techniques. After Ad5/mT cell infection 75% of total mT is normally retained in P100 (at 100,000 xg pelletable fraction) membrane containing fractions (3). Therefore in infected MRC5 cells the Shc associated with mT should redistribute from cytosolic fractions to the P100 fraction.

Uninfected MRC5 cells were grown to ~ 80% confluence, and MRC5 cells for Ad5/mT infection, as described in section 2.6, to ~ 70% confluence. S100 (cytosolic) and P100 fractions of uninfected and of Ad5/mT infected MRC5 cells at 40 hours post infection were obtained as described in 2.6. These fractions were then analyzed for Shc (uninfected cells) or Shc and mT (infected cells) distribution by immunoblotting. Representative results are shown in figure 15 a, b, c.

As expected from previous studies (26), western blot analysis of Shc in uninfected MRC5 total cell lysate, nuclear, cytosolic and membranous fractions showed that the majority of Shc was present in the cytosol. In addition, small amounts of Shc were present in nuclear and membrane fractions (Fig. 15.a). The affinity purified polyclonal antibody to Shc recognized three to four protein bands in MRC5 cells. Molecular weights of these species estimated from mobility in SDS-Page revealed apparent

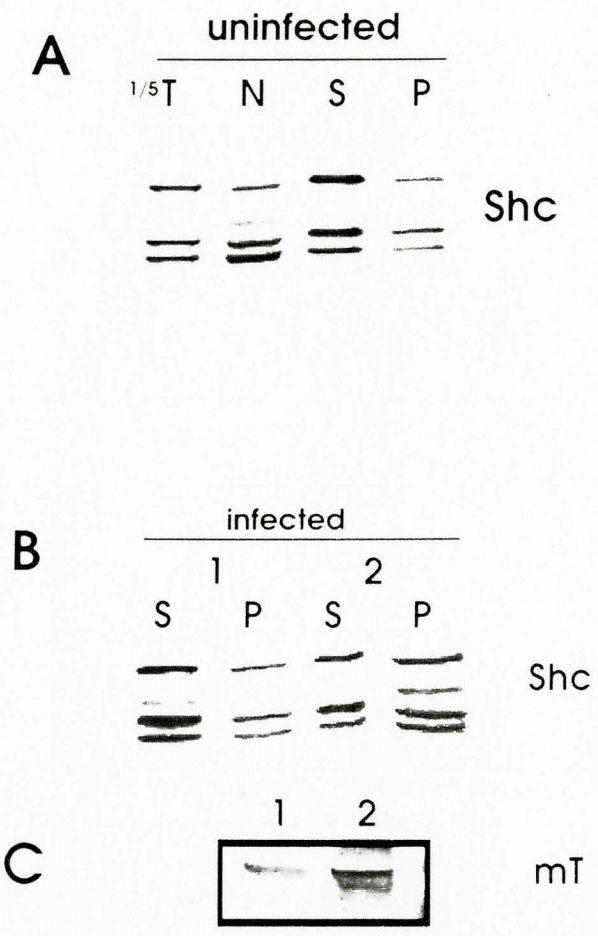

FIG. 15. Western blot analysis of mT and/or Shc distribution in different cell fractions of Ad5/mT infected or uninfected MRC5 cells. Aliquots of different cell fractions from equal number of cells were electrophoretically separated by SDS-Page, transferred to nitrocellulose and probed with primary antibodies to Shc or mT as described in section 2.8. Antibody bands were then detected with anti-rabbit alkaline phosphatase-conjugated antibody. A) Immunoblot of 1/5 of cell lysate (T), nuclear (N), cytosolic (S) and P100 fractions (P) of uninfected cells probed with primary anti-Shc antibody. B) Immunoblot for Shc of cytosolic (S) and P100 fractions (P) from two different preparations (1, 2) of Ad5/mT infected cells expressing different amounts of mT at 40 hours. C) Corresponding membrane fractions (P1, P2) probed with anti-mT antibody.

molecular weights of 62 kDa, 54 kDa, 50 kDa and 47 kDa. The 62 kDa, 50 kDa and 47 kDa proteins were detected in every immunoblot, whereas the expression of the 54 kDa protein varied strongly between the different immunoblots of different cell preparations of Ad5/mT infected MRC5 cells. The 47 kDa, 50 kDa and 62 kDa proteins likely represent the 46 kDa, 52 kDa and 66 kDa Shc isoforms found in other established cell lines (26, 27).

In Ad5/mT infected MRC5 cells, the relative amount of cytosolic and P100 fraction associated Shc varied between different cell preparations (Fig. 15.b) and correlated with the level of cellular mT expression (Fig. 15.b and c). The residual amount of Shc remaining in the S100 fraction is consistent with the results reported above obtained by indirect immunofluorescence. The total Shc in uninfected MRC5 cells was similar to that of infected cells, indicating that an alteration in subcellular localization rather than an increase in total protein accounts for the results. Furthermore the amount of Shc detected in nuclear fractions (probably due to contamination with unbroken cells) of the different preparations from infected and uninfected cells was approximately the same (data not shown).

Using phase partitioning to separate cytoskeletal markers from integral membrane proteins (3, 52), our lab has shown that most of the mT antigen expressed in mT transformed Rat-2 cells and at late times in Ad5/mT infected 293 N3S cells is located in the fraction enriched for membrane skeleton (3). Therefore, we used phase partitioning to examine Shc and mT in P100 fractions of Ad5/mT infected MRC5 cells early in transformation.

The P100 fractions prepared from uninfected and Ad5/mT infected MRC5 cells were solubilized in buffer containing TX-114 and glycerol. Insoluble cytoskeletal components (C) were removed by centrifugation. Phase separation at 30°C was used to separate hydrophobic membrane proteins (in the detergent phase [D]) from luminal contents and membrane skeleton components. A final centrifugation step separated the aqueous phase into predominently soluble hydrophilic proteins (A) and a fraction enriched in membrane skeleton (M).

As a positive control for the correct partitioning of adenovirus vector encoded proteins, the transmembrane rabies G-protein was examined. As expected the protein was found in the detergent phase (D) after phase partitioning (figure 16). Therefore, even when expressed at high levels in adenovirus infected cells, membrane proteins are still found primarily in the detergent fraction after separation by phase partitioning. The enrichment of mT in the membrane skeleton containing fraction is therefore not due to an artifact of overexpression using an adenovirus vector.

After phase partitioning of P100 membrane fractions prepared from Ad5/mT infected MRC5 cells, immunoblotting with affinity purified polyclonal antibody to Shc revealed that most of the protein fractionates in the cytoskeletal fraction (C), with a small amount in the aqueous (A) and in the membrane skeleton (M) fractions (Fig. 17.a). In immunoblots probed with anti-mT antibody, half of mT was detected in the membrane skeleton (M) and half in the cytoskeleton fractions (C) 40 hours after infection (Fig. 17.b).

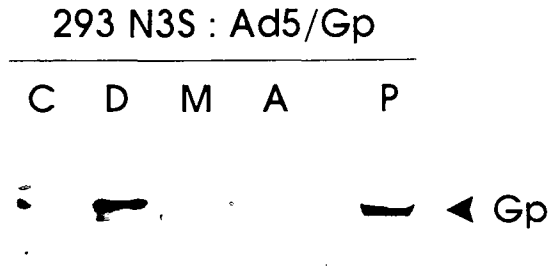

FIG. 16. Western blot analysis of phase partitioning of rabies G-protein. Phase partitionings of Ad5/Gp infected 293 N3S cells were prepared as described in section 2.7. Aliquots were electrophoretically separated by SDS-Page, transferred to nitrocellulose and probed with primary monoclonal antibody to rabies G-protein. Antibody bands were then detected with anti-rabbit alkaline phosphatase-conjugated antibody. Cytoskeleton (C), aqueous (A), membrane skeleton (M) and detergent (D) phase of total P100 (P) of Ad5/Gp infected 293 N3S cells.

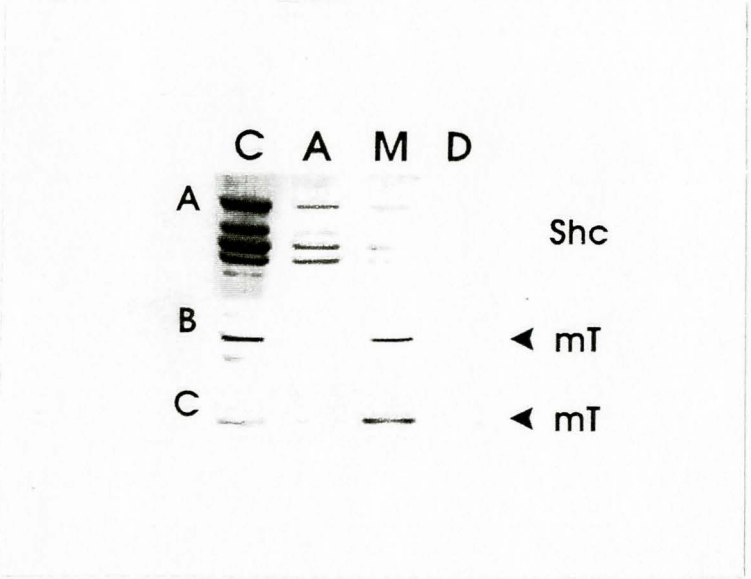

FIG. 17. Western blot analysis of phase partitioning of proteins in infected MRC5 cells at 40 and 48 hours. Phase partitioning of P100 fractions from Ad5/mT infected MRC5 cells were prepared as described in section 2.7. Aliquots were electro-phoretically separated by SDS-Page, transferred to nitrocellulose and probed with primary antibodies to mT or Shc. Antibody bands were then detected with anti-rabbit alkaline phosphatase-conjugated antibody. Immunoblot of cytoskeleton (C), aqueous (A), membrane skeleton (M) and detergent phase (D) probed with primary antibody to Shc at 40 hours (A), with primary anti-mT antibody at 40 hours (B) and at 48 hours (C).

Phase partitioning of membranes prepared from MRC5 cells infected for 48 hours (Fig. 17.c) confirmed our previous data with transformed Rat-2 cells and infected 293 cells (3): almost all of mT was detected in the membrane skeleton fraction (M) and only a small amount of mT was present in the cytoskeleton fraction.

The above results are consistent with the observations made by indirect immunofluorescence. When mT is expressed in MRC5 cells, Shc partly redistributes from the cytosol to a perinuclear structure. Our co-fractionation data suggest Shc redistributes from the cytosol to a cytoskeletal structure in these cells. After phase partitioning of the P100 fraction from Ad5/mT infected MRC5 cells, mT distribution at later times coincides with our previous results in infected 293 N3S cells or Rat-2 cells. At late times, when actin is disassembled as shown by indirect immunofluorescence data, mT is found in the membrane skeleton fraction probably associated with actin containing structures (3). In contrast, at early times, at the onset of mT-transformation and before extensive actin depolymerization mT is found also in the cytoskeleton fraction. Taken together our immunofluorescence data and biochemical analysis provide evidence that there is a difference in intracellular events at early compared to late times after cell transformation is initiated by mT.

4. Discussion

In this study we have demonstrated by indirect immunofluorescence that early in infection of non-transformed embryonal fibroblasts, the vast majority of polyoma mT (mT) antigen is localized to a perinuclear compartment and is not associated with the plasma membrane. In addition, the perinuclear compartment containing mT is distinct from ER, intermediate compartment, Golgi, TGN, secondary lysosomes and late endosomes. Evidence is provided that mT triggers the dismantling of the actin cytoskeleton from this perinuclear location. At later times, secondary lysosomes and late endosomes were reorganized in cells expressing mT. The results also demonstrate partial colocalization of $pp60^{c\text{-}src}$ and mT in coinfected cells, and that perinuclear mT recruits Shc from the cytoplasm to the perinuclear structure. **These results raise the possibility that at this perinuclear localization, mT influences <u>both</u> aspects of cell transformation, namely interfering with mitogenic signalling pathways and alterating cell morphology.**

<u>4.1 MT localization</u>

The location of mT in lytically infected or transformed cells is controversial. Early studies using cell fractionation indicated that 80-95% of polyoma mT antigen is found in plasma membranes (49, 50). This result was consistent with the notion of mT being a membrane associated protein, based

on the presence of a hydrophobic amino acid sequence at the C-terminus (1, 33). In addition, proteins of the mitogenic signalling pathways interact or form complexes with mT (2, 8-20, 23, 25, 27, 65, 71). These proteins are also known to associate and interact with membrane bound growth factor receptors and with other members of the signalling pathways in close proximity to the plasma membrane (88). These observations suggested a model wherein mT molecules interacting with signal transduction proteins were exclusively located at the plasma membrane (38, 88). However, the generality of this model for signal transduction has beeen weakened by the recent observations of intracellular localization of members of the mitogenic signalling pathway. For example, $pp60^{c\text{-}src}$ was found to associate with endosomal membranes in mammalian fibroblasts (38), and mSos, Grb2, phosphotyrosine-modified Shc and phospho-tyrosine activated EGFR were found in rat liver parenchyma endosomes (77). In addition, investigations in lytically infected or transformed cells using indirect immunofluorescence and immuno-electron microscopy support an association of polyoma mT with cytoplasmic membranes, suggested to resemble the Golgi and the ER (34, 110). The data presented in this study show that at the onset of the transformation process, mT is found in a subcellular perinuclear structure distinct from the ER, with no mT detected at the plasma membrane (Fig. 3.a). Small amounts of mT located at plasma membranes are detectable only late in transformation (Fig. 3.e and Fig. 4.a). The reported differences in mT localization can be explained by the fact that previous studies (34, 49, 50) were done in lytically infected or

transformed cells, whereas our results were obtained from a novel cell system using non-transformed cells infected with a viral vector encoding mT antigen. This adenovirus is not capable of replication as the mT coding sequence replaced part of the early viral region needed for replication. Because the vector does not replicate or express viral late proteins, alteration of the cell is minimal. With this system we examined the localization and effects of mT before morphological transformation was complete. Evidence was provided that a similar viral vector encoding the plasma membrane rabies G-protein did not alter cell morphology, confirming that the observed changes are specific for mT (Fig. 3).

Based on sequence homology, it has been postulated that mT is targeted post-translationally to its target membrane via the C-terminal hydrophobic tail (60). However, secretory proteins and proteins found in the plasma membrane normally travel unidirectionally through a vacuolar system that is composed of several membrane-bound compartments (48, 43, 45). Newly synthesized protein enters the system at the endoplasmic reticulum and continues through the cis, medial and trans Golgi cisternae complex, which plays a key role in processing, maturation and sorting (48, 43, 45). The protein then travels to the trans Golgi network (TGN) with the unique function of packing proteins into different types of transport vesicles, from which it can be routed to lysosomes, secretory granules or plasma membrane. The TGN also participates in retrieval and re-utilization of plasma membrane components internalized by endocytosis such as the receptors for mannose-6-

phosphate and transferrin (48, 43, 44, 45). Recently an intermediate compartment (ERGIC) localized between the ER and the Golgi has been described (39, 40). To determine whether mT is localized to one of the above compartments, we stained them with antibodies recognizing compartment specific markers and compared the staining with mT perinuclear localization (Figs. 6 and 7). The possible co-localization of mT with any of the compartment specific proteins was investigated using costains. In addition, we used brefeldin A, a drug that specifically alters certain components of cellular membrane trafficking to disrupt some subcellular compartments.

Staining of cellular markers representing ER, Golgi apparatus, TGN and late endosomes did not coincide with subcellular mT localization (Fig. 6). The only known compartments which partly resembled the staining pattern for mT were the intermediate compartment (FIG. 7/marked by ERGIC-53), and secondary lysosomes and late endosomes (Fig. 9/characterized by the marker LE). Furthermore, mT expression altered the normal staining pattern of secondary lysosomes and late endosomes, an effect not seen when using markers for the other subcellular compartments (Fig. 9). The original distribution of the organelle (over the majority of the cytoplasm in normal cells and early after infection) was changed to a perinuclear and partial plasma membrane staining at later time points after infection (Fig. 9). Therefore secondary lysosomes and late endosomes are reorganized in cells expressing mT; however, mT is unlikely to be located in the plasma membrane and be recycled by endocytosis at the onset of cellular transformation.

The compartment most closely resembling mT staining in uninfected as well as in Ad5/mT infected cells was the intermediate compartment characterized by the marker ERGIC-53 (Fig. 7). However, mT/ERGIC-p53 costaining demonstrated only a partial overlap of both markers in the perinuclear region, as shown by mT and ERGIC-53 staining patterns in inserts (Fig. 7.c and d). To more precisely examine the relationship between mT and ERGIC-53 subcellular localization, we conducted further experiments using the fungal metabolite brefeldin A (BFA).

Previous work with BFA has provided important insights into the dynamics and organization of the ER/Golgi membrane system. BFA treatment of cells has characteristic effects on the structure of the Golgi apparatus, TGN and early endosomes. The ER and intracellular endocytic traffic from the cell surface to the TGN are unaffected by BFA (44). In some cell systems the ERGIC seems to preserve its identity (48), in others, a vesicular distribution of the compartment over the entire cytoplasm takes place (47, 39, 51). The latter observation was made in Vero cells (African green monkey fibroblasts). Therefore, we expected a similar ERGIC-53 distribution in human fibroblasts (MRC5 cells) after BFA treatment. As expected, BFA treatment of human MRC5 fibroblasts resulted in discrete dots of ERGIC-53 staining all over the cytoplasm (Fig. 8), confirming previous BFA data for ERGIC-53 in Vero cells (39, 47). In contrast, there was no change in the distribution of polyoma mT after BFA treatment (Fig. 8). We therefore excluded the possibility that mT is located in the ERGIC-53 containing

intermediate compartment. The above data suggest that if mT is associated with a membrane compartment, it is perinuclear, insensitive to BFA and differs from the ER, TGN and late endosomes, tubular endosomes and the intermediate compartment. Other subcellular compartments do exist, for example, the recently described compartment, distinct from endosomes and lysosomes, which is specialized in the transport and loading of class II MHC molecules in B lymphocytes (54). Therefore we suggest that mT is not located in one of the established vacuolar compartments of the secretory pathway, but in a novel perinuclear structure which is resistant to BFA.

4.2 Implications for mitogenesis

Indirect immunofluorescence with antibodies against pp60$^{c\text{-}src}$ in infected fibroblasts overexpressing the protein revealed a perinuclear distribution with slight plasma membrane staining (Fig. 13), similar to previously published results in a cell line derived from Rat-1 cells infected with a retroviral construct expressing chicken pp60$^{c\text{-}src}$ (38) and in pp60$^{c\text{-}src}$ transfected murine fibroblasts (79). MRC5 cells overexpressing both pp60$^{c\text{-}src}$ and mT showed a partial overlap of staining in the perinuclear area, however, pp60$^{c\text{-}src}$ extended further into the cytoplasm in mT/pp60$^{c\text{-}src}$ costains (Fig. 13). MT also interacts with at least one other member of the mitogenic cellular signalling pathways at this perinuclear location, as Shc is recruited from its usual cytoplasmic distribution (26) to this perinuclear structure after mT expression (Fig. 14). Furthermore treatment with BFA had no effect on this perinuclear Shc

recruitment (Fig. 14).

These results obtained using immunofluorescence were confirmed with immunoblot analysis of cytosolic and membrane cell fractions of Shc (Fig. 15). In uninfected fibroblasts, Shc was found in the cytosolic fraction; in contrast, Shc is found primarily in P100 fractions of cells expressing mT. The amount of Shc redistribution is also correlated with the amount of mT expressed. These results are consistent with recent studies indicating that transformation by mT involves Shc, and that tyrosine phosphorylation of mT (Tyr 250) acts as a binding region for the SH2 domain of Shc (27, 71). Our results suggest that the recruitment of Shc to this perinuclear area by mT is an important aspect of this process.

Shc binds to the growth factor receptor binding protein 2 (Grb2); a homolog of the Drosophila guanine-nucleotide-exchange factor Sos then connects this complex to the Ras signalling pathway (29, 30). MT may initiate activation of this signalling pathway by binding Shc at its specific perinuclear localization, rather than at the plasma membrane. The possibility of activation of the Ras signalling pathway at sites other than the plasma membrane is further supported by the presence of a complex of mSos, Grb2, phosphotyrosine-modified Shc and phosphotyrosine-activated EGFR in endosomes of rat liver parenchyma after exposure to EGF (77). In addition, studies with the v-sis oncogene, which is structurally related to the B chain of platelet-derived growth factor (PDGF), indicate that cell transformation is mediated by internal activation of the PDGFR by v-sis before transport of

either $p28^{v\text{-}sis}$ or the PDGFR to the cell surface (53, 83, 84). Therefore we suggest that mT influences cell transformation by interfering with mitogenic signalling pathways at this perinuclear localization .

4.3 Effect on components of the cytoskeleton

Another aspect of cell transformation is the alteration of cell morphology. Phase partitioning in infected MRC5 cells (Fig. 17) revealed that mT is found attached to the cytoskeleton or in the membrane skeleton fraction at a time when it is localized to the perinuclear area by immunofluorescence (40 hours after infection). Eight hours later, while the majority of mT is still located to perinuclear areas, we observed an increase in the membrane skeleton associated mT, with a concomitant decrease in the cytoskeletal mT (Fig. 17). These results confirmed previous data of a mT sub-population in the membrane skeleton after detergent phase partitioning in transformed Rat-2 and Ad5/mT infected 293 cells (3). The inability to detect mT associated with the cytoskeleton in these cells can be attributed to the fact that the earlier studies were performed in completely transformed cells. Evidence has been presented that transformed fibroblasts have reduced amounts or totally lack actin filaments (102, 103, 91). It seems likely that at the earliest time points of mT cell transformation, more mT is associated with the cytoskeleton than at later time points when the actin cytoskeleton is disassembled. However, at both time points the majority of Shc is associated with the cytokeleton, with only small amounts in the aqueous phase and membrane skeleton phase (Fig.

17).

It was therefore of interest to examine mT interaction with the three classes of filamentous assemblies of the contractile cytoskeleton when localized to the perinuclear area early in infection (Fig. 11). Representative markers for all three classes of the contractile cytoskeleton (actin for microfilaments, vimentin for intermediate filaments and β-tubulin for microtubules) in fibroblasts were found to undergo structural changes during the early stage of mT expression (Fig. 11). In contrast to total actin depolymerization upon cell infection, vimentin and β-tubulin filaments rather appeared to collapse at the the outer cell border with a remaining intact filament network. This data coincides with earlier reports that in viral transformed fibroblasts actin filaments are depolymerized, microtubules can be partly impaired and intermediate filaments remain intact (91, 102, 103, 104, 106). Furthermore, by using a procedure that extracts soluble protein but leaves cytoskeletal elements and associated proteins intact, we demonstated that actin is the primary cytoskeletal target at early stages of mT expression (Fig. 11). Roughly 70% of total mT was extractable with the actin at this time point. In contrast, in Ad5/Gp infected control cells no actin was extractable and therefore no actin depolymerization took place (Fig. 12). This data suggests an interaction of a significant sub-population of mT with specific components of the cytoskeleton.

This interaction may either be a direct mT-actin interaction, or indirect through binding of mT to $pp60^{c\text{-}src}$, $pp60^{c\text{-}src}$ substrates (78, 79), Shc or other

unknown components. Compatible with our results, mitogen induced reorganization of actin filaments has recently been demonstrated in several studies with other growth factor receptors (80, 81, 82). For example, after treatment of A431 cells with epidermal growth factor, the EGF receptor associates through a specific cytoplasmic domain (amino acid residues 984-996) with the actin microfilament system. Similar to the results we have observed, this interaction also alters the microfilament organization.

Other findings that are directly relevant to our results include cofractionation of a mT sub-population in a pp60$^{c\text{-}src}$ dependent manner with the cellular microtubule network in mT transformed rat and mouse cells (63), the association of several pp60$^{c\text{-}src}$ substrates with actin filaments in pp60$^{c\text{-}src}$ transformed chicken embryo cells (78) and in pp60$^{c\text{-}src}$ transfected murine fibroblasts (79), and co-localization of endosomal associated pp60$^{c\text{-}src}$ with the mirotubule organizing center (38). It is possible that the ~30 % mT that is not extractable may be associated with the microtubule organizing center. The pp60$^{c\text{-}src}$ population in endosomes was found to co-localize with the microtubule organizing center (38); this localization changed after treatment with nocodazole, a microtubules depolymerization agent. However, co-fractionation of a sub-population of mT with the cellular microtubule network was <u>not</u> altered upon cell treatment with nocodazole (63). These results are contradictory, but may be explained with different properties or location of vesicles associated with activated mT/pp60$^{c\text{-}src}$ or inactivated pp60$^{c\text{-}src}$ alone (63). Furthermore, both results were obtained in transformed

cells. It is possible that mT interacts with the microtubule organizing center via pp60c-src if examined at the earlier critical time points that we have investigated in our system.

Taken together, these results suggest the following model of mT function: Early in transformation mT interacts with components of the cytoskeleton at a perinuclear localization, thereby producing cell morphology alterations. This mT containing compartment has novel characteristics: It is insensitive to BFA and differs from all other previously recognized structures, including the ER and the intermediate compartment containing the marker ERGIC-53. In addition, at this same location mT may initiate mitogenesis by recruiting members of the cellular signalling pathways. It is very likely that both of these effects are mediated through proteins known to associate with mT or their substrates. Shc and $pp60^{c\text{-}src}$ appear to be involved. Our data raise the possibility that at this perinuclear localization, mT initiates <u>both</u> aspects of cell transformation, namely triggering alterations in cell morphology and interfering with mitogenic signalling pathways.

5. Appendix

5.1 Immunoaffinity purification of polyclonal anti-middle-T serum

Preliminary immunofluorescence results using polyclonal anti-mT serum to localize mT in Ad5/mT infected MRC5 cells indicated that the antiserum had to be further purified, because of high background staining (data not shown). A common strategy to immunoaffinity purify polyclonal antisera is to overexpress the antigen in bacteria, purify large quantities of the pure protein, couple it to CNBr activated Sepharose beads, and then incubate the beads with the antiserum. After several washing steps, fractions enriched in affinity purified antibodies are released with an appropriate buffer. Because a mT-Gst fusion protein was used as the antigen an additional step was included to remove antibodies that bind Gst.

5.1.1 Gst-mT protein overexpression, purification and characterization

Competent cells of the Escherichia coli strain NM522 were transformed with the plasmid pSPGEXmT (made by Gil Abisdris). The plasmid encodes 216 amino acids (aa:176-393) of mT fused to the carboxyl end of glutathione S-transferase (Gst-mT-protein). A saturated culture grown in superbroth (3.2% bactotryptone, 2% yeast extract, 85 mM NaCl, 5 mM NaOH, 100μg/ml ampicillin) was diluted 1:10, incubated for 90 min, then induced with 1 mM final concentration of isopropyl-B-D-Thiogalactopyranoside (IPTG) and grown

for additional 4 hours. The cells were then processed as described previously (61).

For further protein purification, the cell lysate was applied to 2 ml of Glutathione Sepharose (Pharmacia) packed in a 10 ml column (BioRad). The column was washed with 5 bed volumes of phosphate-buffered saline (PBS) and then equilibrated with 3 bed volumes PBS/1% Triton X-100. After loading the cell lysate, the column was washed with 5 volumns of PBS. The remaining Gst-mT fusion protein bound to the Glutathione beads was then eluted with 5 volumns 5 mM reduced Glutathione/50 mM Tris-HCl pH 8.0. The protein content of the collected elution fractions was measured using the Bradford assay (BioRad protein dye reagent).

Figure 18 shows the elution profile of the glutathione column. Most of the fusion protein is contained in fractions two, three, four and five. Fractions one, six, seven, eight, nine and ten contained only minimal quantities of protein, and were discarded.

To analyze the purity of the fusion protein in these fractions, aliquots of these fractions were electrophoretically separated by SDS-Page (62) and proteins stained with Coomassie Blue (figure 19). Two major bands are visible. The upper dominant band of approximately 51 kDa was identified as the desired Gst-mT protein on the basis of expected size and detection by western blot analysis with unpurified mT antiserum (data not shown). The lower also prominent band marked with an asterisk was also seen in untransformed NM522 lysates (data not shown), and is therefore a NM522

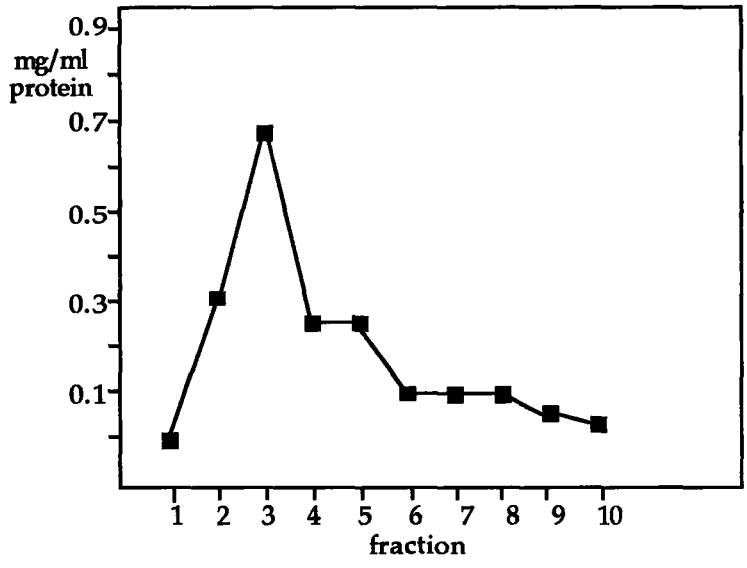

FIG. 18. Glutathione-column elutionprofile of Gst-mT. NM522 cell lysate containing overexpressed Gst-mT fusion protein was applied to a glutathione column. Gst-mT fusion protein was eluted with 5 mM reduced Glutathione, 50 mM tris-HCl pH 8.0, and protein was quantified by Bradford assay.

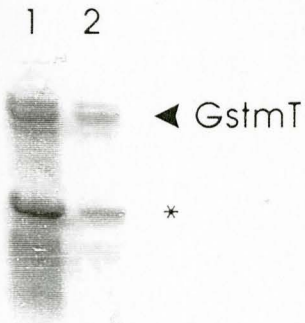

FIG. 19. Analysis of Glutathione column elution fractions three and five. Aliquots of Gst-mT protein elution fractions three and five (lanes 1 and 2) were electrophoretically separated on a SDS-Page and stained with Coomassie Blue.

protein, rather than a Gst-mT degradation product. Protein fractions two to five (total protein yield of ~1.5 mg) were pooled, concentrated with a spin column (Centriprep-10 Concentrator, Amicon), and coupled to hydrated Cyanogen Bromide (CNBr) activated Sepharose (below).

5.1.2 Coupling of Gst or Gst-mT to cyanogen bromide activated Sepharose

Because the serum was raised against the Gst-mT fusion protein, antibodies to gluthathione-S-transferase as well as to mT were present in the serum. To ensure minimal contamination of the purified mT antibodies with Gst antibodies, the crude anti-Gst-mT serum was depleted of anti Gst antibodies by using an immunoaffinity chromatography column containing Gst protein coupled Sepharose. Therefore, both Gst protein and Gst-mT fusion protein were coupled to cyanogen bromide activated Sepharose.

100 mg Cyanogen Bromide (CNBr) activated Sepharose beads (Sigma) were washed 10 times with 1 ml of 10 mM HCl; 0.5 ml of coupling buffer (0.1 M $NaPO_4$ pH 7.0) was added, the slurry was quickly mixed and the beads pelleted by centrifugation. The coupling buffer was then immediately replaced with a protein solution (pH 7.0) containing 1 mg of purified Gst protein (purified by Gil Abisdris) or 1 mg of purified Gst-mT fusion protein. The solution was incubated on a rotating platform at 4^0C for $\geq$ 6 h. After centrifugation, the supernatant was saved for determination of unbound protein by a Bradford assay. 500 μl of 1 M ethanolamine pH 7.5 was added to the beads to block reactive sites and mixed at 4^0C overnight. The following

day the beads were pelleted by centrifugation, the supernatant was discarded and the coupled beads were washed 3 times with 1% Triton X-100/100 mM Tris-HCl pH 8.0/100 mM NaCl/10 mM EDTA.

5.1.3 Immunoaffinity purification of anti-Gst and anti-mT antibodies

Prior to incubation with the serum, the Gst-coupled beads were prepared by washing with different buffers. Buffer A contained 1mM PMSF, 1xPIN (0.1 μg of chymostatin per ml, 0.1 μg of antipain per ml, 0.1 μg of leupeptin per ml, 0.1 μg of pepstatin per ml, 1 U of aprotinin per ml) in PBS. To remove non-covalently attached material, the beads were washed twice with elution buffer (0.2 M glycine pH 2.6). Thereafter the column was washed with buffer C (1mM PMSF, 1xPIN, 0.1 M $NaHCO_3$ pH 8.3, 0.5 m NaCl) and buffer A to establish neutral pH. Serum (3 ml) was diluted with 4 ml PBS and incubated with the beads for 1 hour at 4^0C on a rotating platform. The beads were then packed in a 10 ml propylene econo-chromathography column from BioRad and the serum flowthrough was saved for later incubation with Gst-mT coupled beads. The column was washed with 20 ml of PBS, and bound anti-Gst antibody eluted with 0.2 M glycine pH 2.6. 200 μl fractions were added to 600 μl of 1 M Tris-HCl pH 8.0. Altogether twelve elution fractions with a total protein content of 2.05 mg were collected and stored at -80^0C.

When purified anti-Gst fractions (figure 20.a) were analyzed by immunoblotting (as described in 2.8), a distinct band the size of 32 kDa corresponding to the glutathione S-transferase bound to the nitrocellulose

was present in elution fractions one to nine.

For affinity purification of mT antibodies, Gst-mT coupled CNBr activated Sepharose beads were prepared and treated as described above. To ensure minimal contamination of the purified mT antibodies with Gst antibodies, the beads were incubated with the serum flowthrough of the Gst column. Again twelve elution fractions each 200 μl were collected and added to 600 μl of 1 M Tris-HCl pH 8.0. The antibody concentration of the different elution fractions were quantified by Bradford assay and stored at -80^{0}C. Total yield of anti-mT antibody was 2 mg.

Western blot analysis (slot blot) of fractions from the Gst-mT column, using the P100 fraction of Ad5/mT infected 293 N3S cells as the nitrocellulose bound probe, indicated that significant antibody was present in fractions one to ten (figure 20.b). The major band detected as a doublet in fractions 2-4 may correspond to different modified isomers of mT antigen. The identity of the other bands on the Western blot is unclear; the lower band marked with the small arrowhead may be a degradation product of mT (3), and the upper two bands (+) may be alternate splicing products or readthrough of the termination codon (3). All three of these bands are detected in Western blots of P100 from 293 N3S cells infected with Ad5/mT using a variety of monoclonals to mT. Therefore they are derived from mT and dependent on Ad5/mT infection of 393 N3S cells. However, when this immunoaffinity purified mT antibody was used in Western blot analysis of mT from Ad5/mT infected MRC5 cells as in figure 17.c, only one major reactive product was detectable.

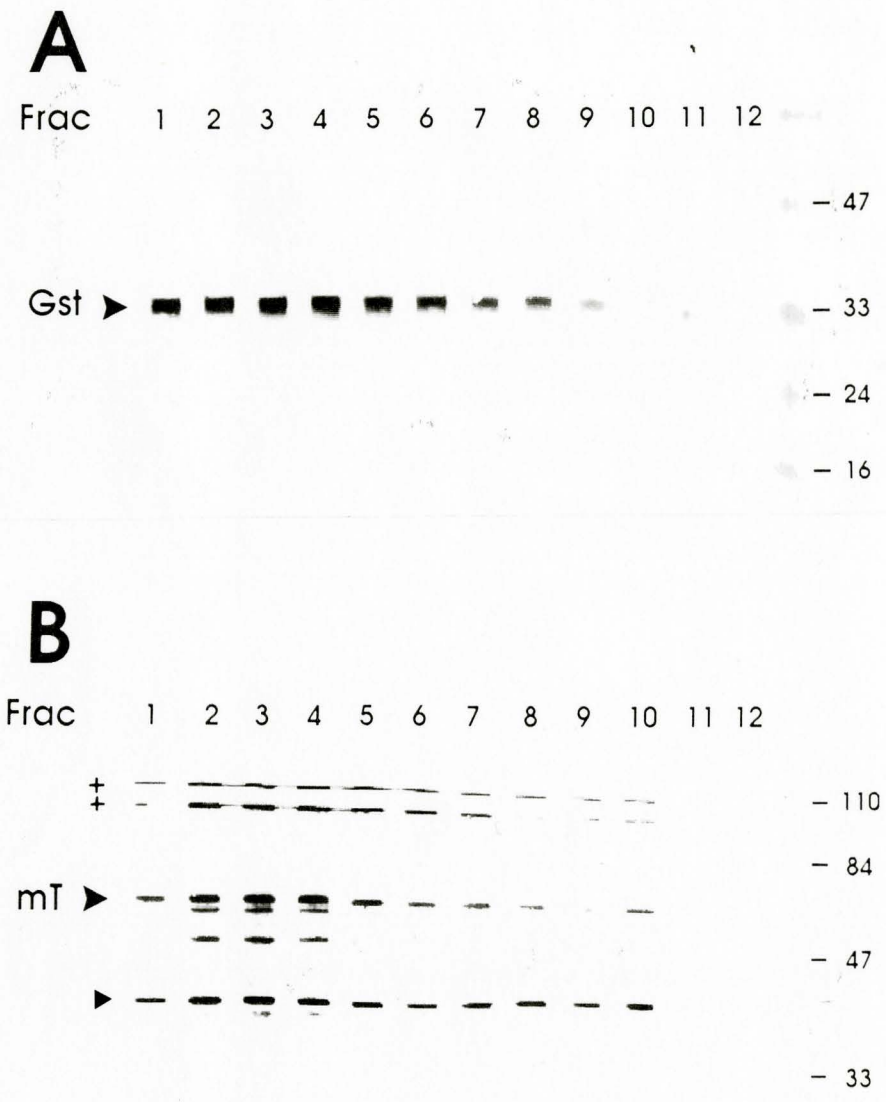

FIG. 20. Western blot analysis of immunoaffinity purified polyclonal anti-Gst (A) and anti-mT (B) antibodies. 2.5 μg of total purified Gst protein (A) and 5 μg total protein of 293 N3S P100 fraction (B) were electrophoretically separated by SDS-Page and transferred to nitrocellulose. The resulting blots were probed on a slot blot apparatus with aliquots of the elution fractions (diluted 1/50 in polyclonal antibody buffer). Antibody bands were detected with anti-rabbit alkaline phosphatase-conjugated antibodies.

6. References

(1) Griffin, B. G. and Dilworth, S. M. 1983. Polyomavirus: an overview of its unique properties. **Adv. Cancer Res.** 39: 183-268.

(2) Kaplan, D. R., Pallas, D. C., Morgan, W., Schaffhausen, B., and Roberts, T. M. 1988. Mechanisms of transformation by Polyoma middle T antigen. **Biochem. Biophys. Acta** 948: 345-364.

(3) Andrews, D. W., Gupta, J. and Abisdris, G. 1993. Evidence that the middle T antigen of polyomavirus interacts with the membrane skeleton. **Mol. Cell. Biol.** 13: 4703-4713.

(4) Pallas, D., Cherington, V., Morgan, W., DeAnda, J., Kaplan, D., Schaffhausen, B. and Roberts, T. M. 1988. Cellular proteins that associate with the middle and small T antigens of polyomavirus. **J.Virol.** 62: 3934-3940.

(5) Cook, D. N. and Hassell, J. A. 1990. The amino terminus of polyomavirus middle T antigen is required for transformation. **J. Virol.** 64: 1879-1887.

(6) Serunian, L. A., Auger, K. R., Roberts, T. M. and Cantley, L. C. 1990. Production of novel polyphosphoinositides in vivo is linked to cell transformation by polyoma middle T antigen. **J.Virol.** 64: 4718-4725.

(7) Berkner, K. L., Schaffhausen, B. S., Roberts, T. M. and Sharp, P. A. 1987. Abundant expression of polyomavirus middle T antigen and dihydrofolate reductase in an adenovirus recombinant. **J. Virol.** 61: 1213-1220.

(8) Courtneidge, S. A. and Smith, A. E. 1983. Polyoma virus transforming protein associates with the product of the c-src cellular gene. **Nature (Lond.)** 303: 435-439.

(9) Cheng, S. H., Piwnica-Worms, H., Harvey, R. W., Roberts, T. M. and Smith, A. E. 1988. The carboxy terminus of pp60$^{c\text{-}src}$ is a regulatory domain and is involved in complex formation with the middle-T antigen of polyomavirus. **Mol. Cell. Biol.** 8: 1736-1747.

(10) Piwnica-Worms, H., Williams, N. G., Cheng, S. H. and Roberts, T. M. 1990. Regulation of pp60$^{c\text{-}src}$ and its interaction with polyomavirus middle T antigen in insect cells. **J. Virol.** 64: 61-68.

(11) Kornbluth, S., Sudol, M. and Hanafusa, H. 1987. Association of the polyomavirus middle-T antigen with c-yes protein. **Nature (Lond.)** 325: 171-173.

(12) Kornbluth, S., Markland, W., Fukui, Y. and Hanafusa, H. 1990. Association of $p62^{c\text{-}yes}$ with polyomavirus middle T-antigen mutants correlates with transforming ability. **J. Virol. 64:** 1584-1589.

(13) Cheng, S. H., Harvey, R., Espino, P. C., Semba, K., Yamamoto, T., Toyoshima, K. and Smith, A., 1988. Peptide antibodies to the human c-fyn gene product demonstrate $pp59^{c\text{-}fyn}$ is capable of complex formation with the middle-T antigen of polyomavirus. **EMBO J.** 7: 3845-3855.

(14) Horak, I. D., Kawakami, T., Gregory, F., Robbins, K. C. and Bolen, J. B. 1989. Association of $p60^{fyn}$ with middle tumor antigen in murine polyomavirus-transformed rat cells. **J. Virol.** 63: 2343-2347.

(15) Cheng, S., Espino, P. C., Marshall, J. H., Harvey, R., Merrill, J. and Smith, A. E. 1991. Structural elements that regulate $pp59^{c\text{-}fyn}$ catalytic activity, transforming potential, and ability to associate with polyoma middle-T antigen. **J. Virol.** 65: 170-179.

(16) Auger, K. R., Carpenter, CH. L., Shoelson, S. E., Piwnica-Worms, H. and Cantley, L. C. 1992. Polyoma virus middle T antigen-$pp60^{c\text{-}src}$ complex associates with purified phosphatidylinositol 3-kinase in vitro. **J. Biol. Chem.** 267: 5408-5415.

(17) Yoakim, M., Hou, W., Liu, Y., Carpenter, Ch. L., Kapeller, R. and Schaffhausen, B. 1992. Interactions of polyoma middle T with the SH2 domains of the pp85 subunit of phosphatidylinositol 3-kinase. **J. Virol.** 66: 5485-5491.

(18) Cohen, B., Liu, Y., Druker, B., Roberts, T. M. and Schaffhausen, B. 1990. Characterization of pp85, a target of oncogenes and growth factor receptors. **Mol. Cell. Biol.** 10: 2909-2915.

(19) Holt, K. H., Olson, A.-L., Moye-Rowley, W. S. and Pessin, J. E. 1994. Phosphatidylinositol 3-kinase activation is mediated by high-affinity interactions between distinct domains within the pp110 and pp85 subunits. **Mol. Cell. Biol.** 14: 42-49.

(20) Klippel, A., Escobedo, J. A., Hirano,. M. and Williams, L. 1994. The interaction of small domains between the subunits of phosphatidylinositol 3-kinase determines enzyme activity. **Mol. Cell. Biol.** 14: 2675-2685.

(21) Gorga, F. G., Riney, C. E. and Benjamin, T. L. 1990. Inositol triphosphate levels in cells expressing wild-type and mutant polyoma middle t antigens: Evidence for activation of phospholipase C via activation of pp60$^{c\text{-}src}$. **J. Virol.** 64: 105-112.

(22) Thomas, J. E., Aguzzi, A., Soriano, P., Wagner, E. F. and Brugge, J. S. 1993. Induction of tumor formation and cell transformation by polyoma middle t antigen in the absence of Src. **Oncogene** 8: 2521-2529.

(23) Pallas, D. C., Sharrik, L. K., Martin, B. L., Jaspers, S., Miller, T. B., Brautigan, D. L. and Roberts, T. M. 1990. Polyoma small and middle T antigens and SV40 small t antigen form stable complexes with protein phosphatase 2A. **Cell** 60: 167-176.

(24) Ulug, E. T., Cartwright, A. J. and Courtneidge, S. A. 1992. Characterization of the interaction of polyoma middle T antigen with type 2A protein phosphatase. **J. Virol.** 66: 1458-1467.

(25) Dilworth, S. M. and Horner, V. P. 1993. Novel monoclonal antibodies that differenciate between the binding of pp60c-src or protein phosphatase 2A by polyoma middle T antigen. **J. Virol.** 67: 2235-2244.

(26) Pelicci, G., Lanfrancone. L., Grignani, F., McGlade, J., Cavallo, F., Forni, G., Nicoletti, I., Grignani, F., Pawson, T. and Pelicci, P. G. 1992. A novel transforming protein (SHC) with an SH2 domain is implicated in mitogenic signal transduction. **Cell** 70: 93-104.

(27) Dilworth, S. M., Brewster, C. E. P., Jones, M. D., Lanfrancone, L., Pellici, G. and Pellici, P. G. 1994. Transformation by polyoma middle T-antigen involves the binding and tyrosine phosphorylation of Shc. **Nature (Lond.)** 367: 87-90.

(28) Rozakis-Adcock, M., McGlade, J., Mbamalu, G., Pellici, G., Batzer, A., Thomas, S., Brugge, J., Pellici, P. G., Schlessinger, J. and Pawson, T. 1992. Association of the Shc and Grb2/Sem5 SH2-containing proteins is implicated in activation of the Ras pathway by tyrosine kinases. **Nature (Lond.)** 360: 689-692.

(29) Egan, S. E., Giddings, B. W., Brooks, M. W., Buday, L., Sizeland, A. M. and Weinberg, R. A. 1993. Association of Sos Ras exchange protein with Grb2 is implicated in tyrosine kinase signal transduction and transformation. **Nature (Lond.)** 363: 45-51.

(30) Lowenstein, E. J., Daly, R. J., Batzer, A. G., Li, W., Margolis, B., Lammers, R., Ullrich, A., Skolnik, E. Y., Bar-Sagi, D. and Schlessinger, J. 1992. The SH2 and SH3 domain-containing protein GRB2 links receptor tyrosine kinases to ras signaling. **Cell** 70: 431-442.

(31) Glenn, G. M. and Eckhart, W. 1993. Mutation of a cysteine residue in polyomavirus middle T antigen abolishes interactions with the protein phosphatase 2A, pp60$^{c\text{-}src}$, and phosphatidylinositol 3-kinase, activation of c-fos expression, and cellular transformation. **J. Virol.** 67: 1945-1952.

(32) Markland, W. and Smith, A. E. 1987. Mutants of poyoma middle T antigen. **Biochem. Biophys. Acta** 907: 299-321.

(33) Carmichael, G. G., Schaffhausen, B. S., Dorsky, D. I., Oliver, D. B. and Benjamin, T. L. 1982. Carboxy terminus of polyoma middle-sized tumor antigen is required for attachment to membranes, associated protein kinase activities, and cell transformation. **Proc. Natl. Acad. Sci. USA.** 79: 3579-3583.

(34) Dilworth, S. M., Hansson, H.-A., Danfors, C., Bjursell, G., Streuli, C. H. and Griffin, B. E. 1986. Subcellular localisation of the middle and large T-antigens of polyoma virus. **EMBO J.** 5: 491-499.

(35) Cook, D. N., Pavloff, N. and Hassell, J. A. 1990. Simultaneous overexpression of avian pp60$^{c\text{-}src}$ and polyomavirus middle T antigen in mammalian cells. **J. Virol.** 64: 2392-2395.

(36) Takemoto, K. K., Malmgren, R. A. and Habel, K. 1966. Immuno-fluorescence demonstration of polyoma tumor antigen in lytic infection of mouse embryo cells. **Virology** 28: 485-488.

(37) Louvard, D., Reggio, H. and Warren, G. 1982. Antibodies to the Golgi complex and the rough endoplasmatic reticulum. **J. Cell. Biol.** 92: 92-107.

(38) Kaplan, K. B., Swedlow, J. R., Varmus, H. E. and Morgan, D. O. 1992. Association of p60c-src with endosomal membranes in mammalian fibroblasts. **J. Cell. Biol.** 118: 321-333.

(39) Schweizer, A., Fransen, J. A. M., Matter, K., Kreis, T. E., Ginsel, L. and Hauri, H.-P. 1990. Identification of an intermediate compartment involved in protein transport from endoplasmatic reticulum to Golgi apparatus. **Eur. J. Cell. Biol.** 53: 185-196.

(40) Hauri, H.-P. and Schweizer, A. 1992. The endoplasmic reticulum-Golgi intermediate compartment. **Cur. Op. in Cell Biol.** 4: 600-608.

(41) Schweizer, A., Peter, F., Nguyen Van, P., Soeling, H.-D. and Hauri, H.-P. 1992. A luminal calcium-binding protein with a KDLE endoplasmic reticulum retention motif in the ER-Golgi intermediate compartment. **Eur. J. Cell. Biol.** 60: 366-370.

(42) Schindler, R., Itin, Ch., Zerial, M., Lottspeich, F. and Hauri, H.-P 1993. ERGIC-53, a membrane protein of the ER-Golgi intermediate compartment, carries an ER retention motif. **Europ. J. Cell. Biol.** 61: 1-9.

(43) Klausner, R. D., Donaldson, J. G. and Lippincott-Schwarz, J. 1992. Brefeldin A: insights into the control of membrane traffic and organelle structure. **J. Cell. Biol.** 116: 1071-1080.

(44) Miller, S. G., Carnell, L. and Moore, H.-P. H. 1992. Post-Golgi membrane traffic: Brefeldin A inhibits export from distal Golgi compartments to the cell surface but not recycling. **J. Cell. Biol.** 118: 267-283.

(45) Reaves, B. and Banting, G. 1992. Perturbation of the morphology of the trans-Golgi network following Brefeldin A treatment: Redistribution of a TGN-specific integral membrane protein, TGN 38. **J. Cell. Biol.** 116: 85-94.

(46) Wood, S. and Brown, W. J. 1992. The morphology but not the function of endosomes and lysosomes is altered by Brefeldin A. **J. Cell. Biol.** 119: 273-285.

(47) Schweizer, A., Clausen, H., van Meer, G. and Hauri, H.-P. 1994. Localization of O-glycan initiation, sphingomyelin synthesis, and glucosylceramide synthesis in Vero cells with respect to the endoplasmic reticulum-Golgi intermediate compartment. **J. Biol. Chem.** 269: 4035-4041.

(48) Rios, R. M., Tassin, A.-M., Celati, C., Antony, C., Boissier, M.-C., Homberg, J.-C. and Bornens, M. 1994. A peripheral protein associated with the cis-Golgi network redistributes in the intermediate compartment upon Brefeldin A treatment. **J. Cell. Biol.** 125: 997-1013.

(49) Ito, Y., Brocklehurst, J. R. and Dulbecco, R. 1977. Virus-specific proteins in the plasma membrane of cells lytically infected or transformed by polyoma virus. **Proc. Natl. Acad. Sci. USA.** 74: 4666-4670.

(50) Segawa, K. and Ito, Y. 1982. Differential subcellular localization of in vivo-phosphorylated and nonphosphorylated middle-sized tumor antigen of polyoma virus and its relationship to the middle-sized tumor antigen phosphorylating activity in vitro. **Proc. Natl. Acad. Sci. USA.** 79: 6812-6816.

(51) Lippincott-Schwarz, J., Donaldson, J. G., Schweizer, A., Berger, E. G., Hauri, H.-P., Yuan, L. C. and Klausner, R. D. 1990. Microtubule-dependent retrograde transport of proteins into the ER in the presence of Brefeldin A suggests an ER recycling pathway. **Cell** 60: 821-836.

(52) Bordier, C. 1981. Phase separation of integral membrane proteins in Triton X-114 solution. **J. Biol. Chem.** 256: 1604-1607.

(53) Lee, B. A. and Donoghue, D. J. 1992. Intracellular retention of membrane-anchored v-sis protein abrogates autocrine signal transduction. **J. Cell Biol.** 118: 1057-1070.

(54) Amigorena, S., Drake, J. R., Webster, P. and Mellman, I. 1994. Transient accumulation of new class II MHC molecules in a novel endocytic compartment in B lymphocytes. **Nature (Lond.)** 369: 113-120.

(55) Davidson, D. and Hassell, J. A. 1987. Overproduction of polyomavirus middle T antigen in mammalian cells through use of an adenovirus vector. **J. Virol.** 61: 1226-1239.

(56) Jelinek, M. A. and Hassell, J. A. 1992. Reversion of middle T antigen-transformed Rat-2 cells by Krev-1: implications for the role of $p21^{c\text{-}ras}$ in polyoma-mediated transformation. **Oncogene** 7: 1687-1698.

(57) Pallas, D. C., Fu, H., Haehnel, L. C., Weller, W., Collier, R. J. and Roberts T. M. 1994. Association of polyoma middle tumor antigen with 14-3-3 proteins. **Science** 265: 535-537.

(58) Aitken, A., Collinge, D. B., van Heusden, B. P. H., Isobe, T., Roseboom, P. H., Rosenfeld, G. and Soll, J. 1992. 14-3-3 proteins: a highly conserved, widespread family of eukaryotic proteins. **Trends Biochem. Sci.** 17: 498-501.

(59) Soeda, E., Arrand, J. R., Smolar, N., Walsh., E. and Griffin, B. E. 1980. Coding potential and regulatory signals of the polyoma virus genome. **Nature (Lond.)** 283: 445-453.

(60) Sabatini, D. D., Kreibich, G., Morimoto, T. and Adesnick, M. 1982. Mechanisms for the incorporation of proteins in membranes and organelles. **J. Cell Biol.** 92: 1-22.

(61) Lin, K.-H. and Cheng, S.-Y. 1991. An efficient method to purify active eukaryotic proteins from the inclusion bodies in Escherichia coli. **BioTechniques** 6: 748-753.

(62) Schagger,H. and Von Jagow, G. 1987. Tricine-sodium dodecyl sulphate-polyacrylamid gel electrophoresis for the separation of proteins in the range from 1-100 kDa. **Anal. Biochem.** 166: 368-379.

(63) Krauzewicz, N., Elliott, J. and Griffin, B. E. 1994. Cell fractionation in non-ionic detergent distinguishes sub-populations of polyoma virus middle T antigen and reveals a novel form. **Oncogene** 9: 2283-2291.

(64) Folkman, J., Moscona, A., 1978. Role of cell shape in growth control. **Nature (Lond.)** 273: 345-349.

(65) Cooper, J. and Howell, B. 1993. The when and how of Src regulation. **Cell** 73: 1051-1054.

(66) Musacchio, A., Gibson, T., Letho, V.-P. and Saraste, M. 1992. SH3- an abundant protein domain in search of a function. **FEBS Lett.** 307: 55-61.

(67) Mayer, B. J. and Baltimore, D. 1993. Signalling through SH2 and SH3 domains. **Trends in Cell Biol.** 3: 8-13.

(68) Weng, Z., Thomas, S. M., Rickles, R. J., Taylor, J. A., Brauer, A. W., Seidel-Dugan, C., Miachael, W. M., Dreyfuss, G. and Brugge, J. S. 1994. Identification of Src, Fyn, and Lyn SH3- binding proteins: Implications for a function of SH3 domains. **Mol. Cell. Biol.** 14: 4509-4521.

(69) Panayotou, G. and Waterfield, M. D. 1992. Phosphatidylinositol 3-kinase: a key enzyme in divers signalling processes. **Trends in Cell Biol.** 2: 358-360.

(70) Parker, P. J. and Waterfield M. D. 1992. Phosphatidylinositol 3-kinase: a novel effector. **Cell Growth & Differentiation** 3: 747-752.

(71) Campbell, K. S., Ogris, E., Burke, B., Su, W., Auger, K. R., Druker, B. J., Schaffhausen, B. S., Roberts, T. M. and Pallas, D. C. 1994. Polyoma middle tumor antigen interacts with Shc protein via the NPTY (Asn-Pro-Thr-Tyr) motif in middle tumor antigen. **Proc. Natl. Acad. Sci. USA.** 91: 6344-6348.

(72) Alberts, B., Bray, D., Lewis, J., Raff, M., Roberts, K. Watson, J. D. 1989. **Molecular Biology of The Cell.** 2 nd. ed. Garland Publishing, Inc. New York & London: 282, 702-704.

(73) Bar-Sagi, D., Rotin, D., Batzer, A., Mandiyan, V. and Schlessinger, J. 1993. SH3 domains direct cellular localization of signaling molecules. **Cell** 74: 83-91.

(74) Cooper, J. A. 1987. Effects of cytochalasin and phalloidin on actin. **J. Cell Biol.** 105: 1473-1478.

(75) Luzio, J. P., Brake, B., Banting, G., Howell, K. E. and Braghetta, F. 1990. Identification, sequencing, and expression of an integral membrane protein of the trans-Golgi network (TGN-38). **Biochem. J.** 270: 97-102.

(76) Saraste, J., Palade, G. E and Farquhar, M. G. 1987. Antibodies to rat pancreas Golgi subfractions: Identification of a 58-kD cis-Golgi protein. **J. Cell Biol.** 105: 2021-2029.

(77) Di Guglielmo, G. M., Baass, P. C., Ou, W.-J., Posner, B. I. and Bergeron, J. J. M. 1994. Compartmentalization of Shc, GRB2 and mSOS, and hyperphosphorylation of RAF-1 by EGF but not insulin in liver parenchyma. **EMBO J.** 13: 4269-4277.

(78) Flynn, D. C., Leu, T-H, Reynolds, A. B. and Parsons, J. T. 1993. Identification and sequence analysis of cDNAs encoding a 110-kilodalton actin filament-associated pp60$^{c\text{-}src}$ substrate. **Mol. Cell. Biol.** 13: 7892-7900.

(79) Maa, M.-C., Wilson, L. K., Moyers, J. S., Vines, R. R., Parsons, J T. and Parsons, S. J. 1992. Identification and characterization of a cytoskeleton-associated, epidermal growth factor sensitive pp60$^{c\text{-}src}$ substrate. **Oncogene** 7: 2429-2438.

(80) Den Hartigh, J. C., van Bergen en Henegouwen, P. M. P., Verkleij, A. J. and Boonstra, J. 1992. The EGF receptor is an actin-binding protein. **J. Cell Biol.** 119: 349-355.

(81) Peppelenbosch, M. P., Tertoolen, L. G. J., Hage, W. J. and de Laat, S. W. 1993. Epidermal growth factor-induced actin remodeling is regulated by 5-lipoxygenase and cyclooxygenase products. **Cell** 74: 565-575.

(82) Rijken, P. J., Hage, W. J., van Bergern en Henegouwen, P. M. P., Verkleij, A. J. and Boonstra, J. 1991. Epidermal growth factor induces rapid reorganization of the actin microfilament system in human A431 cells. **J. Cell Sci.** 100: 491-499.

(83) Keating, M. T. and Williams, L. T. 1988. Autocrine stimulation of intracellular PDGF receptors in v-sis-transformed cells. **Science** 239: 914-916.

(84) Bejcek, B. E., Li, D. Y. and Deubel, T. F. 1989. Transformation by v-sis occurs by an internal autoactivation mechanism. **Science** 245: 1496-1499.

(85) Ballmer-Hofer, K. and Benjamin, T. L. 1985. Phosphorylation of polyoma middle T antigen and cellular proteins in purified plasma membranes of polyoma virus-infected cells. **EMBO J.** 4: 2321-2327.

(86) Treisman, R., Novak, U., Favaloro, J. and Kamen, R. 1981. Transformation of rat cells by an altered polyoma virus genome expressing only the middle-T protein. **Nature (Lond.)** 292: 595-600.

(87) Rassoulzadegan, M., Courtneidge, S., Loubiere, R., El Baze, R. and Cuzin, F. 1990. A variety of tumors induced by middle T antigen of polyoma virus in a transgenic mouse family. **Oncogene** 5: 1507-1510.

(88) Ullrich, A. and Schlessinger, J. 1990. Signal transduction by receptors with tyrosine kinase activity. **Cell** 61: 203-212.

(89) Donaldson, J. G., Lippincott-Schwartz, J., Bloom, G. S., Kreis, T. E. and Klausner, R. D. 1990. Dissociation of a 110-kD peripheral membrane protein from the Golgi apparatus is an early event in Brefeldin A action. **J. Cell Biol.** 111: 2295-2306.

(90) Darnell, J., Lodish, H. and Baltimore, D. 1990. **Molecular Cell Biology.** 2nd ed. Scientific American Books: 955-998.

(91) Ben-Ze`ev, A. 1985. The cytoskeleton in cancer cells. **Biochem. Biophys. Acta** 780: 197-212.

(92) Burridge, K., Fath, K., Kelly, T., Nuckolls, G. and Turner, C. 1988. Focal adhesions: Transmembrane junctions between the extracellular matrix and the cytoskeleton. **Ann. Rev. Cell Biol.** 4: 487-525.

(93) Luna, E. J. and Hitt, A. L. 1992. Cytoskeleton-plasma membrane interactions. **Science** 258: 955- 964.

(94) Sefton, B. M. and Hunter T. 1981. Vinculin: a cytoskeletal target of the transforming protein of Rous Sarcoma Virus. **Cell** 24: 165-174.

(95) Jove, R. and Hanafusa, H. 1987. Cell transformation by the viral src oncogene. **Ann. Rev. Cell Biol.** 3: 31-56.

(96) Hu, P., Mondino, A., Skolnik, E. Y. and Schlessinger, J. 1993. Cloning of a novel, ubiquitously expressed human phosphatidylinositol 3-kinase and identification of its binding site on p85. **Mol. Cell. Biol.** 13: 7677-7688.

(97) Markland, W., Oostra, B. A., Harvey, R., Markham, A. F., Colledge, W. H. and Smith, A. E. 1986. Site-directed mutagenesis of polyoma middle-T antigen sequences encoding tyrosine 315 and tyrosine 250. **J. Virol.** 59: 384-391.

(98) Redmond, T., Brott, B. K., Jove, R. and Welsh, M., J. 1992. Localization of the viral and cellular src kinase to the perinuclear vesicles in fibroblasts. **Cell Growth & Differentiation** 3: 567-576.

(99) Cantley, L. C., Auger, K. R., Carpenter, C., Duckworth, B., Graziani, A., Kapeller, R. and Soltoff, S. 1991. Oncogenes and signal transduction. **Cell** 64: 281-302.

(100) Feig, L. A. and Schaffhausen, B. 1994. The hunt for Ras targets. **Nature (Lond.)** 370: 508-509.

(101) Carley, W. W., Barak, L. S. and Webb, W. W. 1981. F-actin aggregates in transformed cells. **J. Cell Biol.** 90: 797-802.

(102) Tucker, R. W. and Sanford, K. K. 1978. Tubulin and actin in paired nonneoplastic and spontaneously transformed neoplastic cell lines in vitro: fluorescent antibody studies. **Cell** 13: 629-642.

(103) Boschek, C. B., Jockusch, B. M., Friis, R. R., Back, R., Grundmann, E. and Bauer, H. 1981. Early changes in the distribution and organization of microfilament proteins during cell transformation. **Cell** 24: 175-184.

(104) Ostlund, R. and Pastan, I. 1975. Fibroblast tubulin. **Biochemistry** 14: 4064-4068.

(105) Chafouleas, J. G., Pardue, R. L., Brinkley, B. R., Dedman, J. R. and Means, A. R. 1981. Regulation of intracellular levels of calmodulin and tubulin in normal and transformed cells. **Proc. Natl. Acad. Sci. USA.** 78: 996-1000.

(106) Brinkley, B. R., Fuller, G. M. and Highfield, D. P. 1975. Cytoplasmic microtubules in normal and transformed cells in culture: analysis by tubulin antibody immunofluorescence. **Proc. Natl. Acad. Sci. USA.** 72: 4981-4985.

(107) Pelham, H. R. B. 1994. About turn for the COPs ?. **Cell** 79: 1125-1127.

(108) Fu, H., Xia, K., Pallas, D., Cui, C., Conroy, K., Narsimhan, R. P., Mamon, H., Collier, R. J. and Roberts, T. M. 1994. Interaction of the protein kinase Raf-1 with the 14-3-3 proteins. **Science** 266: 126-129.

(109) Fantl, W. J., Muslin, A. J., Kikuchi, A., Martin, J. A., MacNichol, A. M., Gross, R. W. and Williams, L. T. 1994. Activation of Raf-1 by 14-3-3 proteins. **Nature (Lond.)** 371: 612-614.

(110) Zhu, Z., Veldman, G. M., Cowie, A., Carr, A., Schaffhausen, B. and Kamen, R. 1984. Construction and functional characterization of polyoma-virus genomes that separately encode the three early proteins. **J. Virol.** 51: 170-180.

(111) Bradford, M. 1976. A rapid and sensitive method for the quantification of microgram quantities of protein utilizing the principle of protein-dye binding. **Anal. Biochem.** 72: 248-252.

(112) Timmons M. S. and Witte, O. N. 1989. Structural characterization of the BCR gene product. **Oncogene** 4: 559-567.